AD 290 619

NOLTR 62-125 JULY 16, 1962

THE APPLIED PHYSICS DEPARTMENT

SOLID STATE RESEARCH FOR THE YEAR 1961

UNITED STATES NAVAL ORDNANCE LABORATORY, WHITE OAK, MARYLAND

SOLID STATE RESEARCH
OF
THE APPLIED PHYSICS DEPARTMENT
FOR THE YEAR 1961

ABSTRACT: Emphasis has been placed upon the optical and electrical properties of the lead salt semiconductors and work on the compound SnTe. Surface transport studies of semiconductors were clarified by a reformulation of the Boltzmann equation. Magnetoelastic interactions constituted an important effort during the year. Acoustic investigations of SiO_2 were continued with reference to the Si-O-Si bond that included the relationships between specific heat and temperature dependence of the elastic moduli of SiO_2 glass. Laser mechanisms have been studied by the use of high speed photography. A new alloy, Nitinol, revealed many unusual properties. Certain device applications of solid state principles are reported.

U. S. NAVAL ORDNANCE LABORATORY
WHITE OAK, MARYLAND

THE STAFF

D. F. Bleil, Associate Director for Research

W. C. Wineland, Physics Program Chief

Applied Physics Department

L. R. Maxwell, Department Chief

W. W. Scanlon, Senior Research Physicist

Divisions

Magnetism and Metallurgy - E. Adams, Chief
Solid State - H. W. McKee, Chief

Consultants

C. G. Shull
R. M. Thomson
R. J. Maurer
P. H. Miller, Jr.
R. M. Bozorth
R. C. Barker

Intermittent Staff

E. C. Treacy
R. A. Ferrell
P. L. Edwards
S. L. Strong

Molecular Magnetism in Solids

E. R. Callen
E. S. Dayhoff
S. J. Pickart
H. A. Alperin
A. E. Clark
B. F. DeSavage
B. V. Kessler
E. P. Wenzel
R. G. Petersen
J. Lamberth
H. T. Savage

Imperfections in Solids

R. E. Strakna
R. J. Happel, Jr.
S. F. Bell

Semiconductors

R. S. Allgaier
F. Bis
R. F. Brebrick
J. R. Burke, Jr.
J. L. Davis
J. R. Dixon
J. Ellis
R. F. Greene
E. Gubner
B. B. Houston, Jr.
J. Jensen
M. K. Norr
H. R. Riedl
E. J. Scott
J. O. Varela
J. N. Zemel
J. F. Goff
F. Stern

Structural Intermetallic Compounds
- W. J. Buehler
- R. C. Wiley
- R. E. Predmore
- A. M. Syeles
- H. E. Eberly
- C. E. Sutton

Soft Magnetic Alloys
- H. H. Helms, Jr.
- E. F. Heintzelman
- J. G. Stewart
- C. G. Reed
- L. B. Higdon

High Energy Particle Irradiation Effects
- R. S. Sery

Ultra-High Pressure Effects
- D. W. Ernst
- M. Pasnak
- J. D. Grimsley

Microwave Spectroscopy
- E. T. Hooper, Jr.
- A. D. Krall
- O. J. Van Sant

Electromagnetic Devices
- W. A. Geyger

Magnetization of Rare Earth Compounds
- W. M. Hubbard
- D. W. Ernst
- R. E. Brown
- J. V. Gilfrich
- L. A. DeVivo
- J. F. Haben

Barkhausen Noise
- D. I. Gordon
- R. H. Lundsten

The Applied Physics Department reports, for the year 1961, on its accomplishments in the field of solid state research which was supported by Foundational Research and project funds provided for by the U. S. Bureau of Naval Weapons.

R. E. ODENING
Captain, USN
Commander

Louis R. Maxwell

L. R. MAXWELL
By direction

CONTENTS

ILLUSTRATIONS

TABLES

MATERIALS REPORT FOR THE APPLIED PHYSICS DEPARTMENT

INTRODUCTION

Our solid state research program continued its emphasis upon the electrical and optical properties of the lead salt semiconductors and intermetallic compound semiconductors with an increasing interest in the compound SnTe. Optical methods for studying energy bands in semiconductors received greater emphasis as a result of the development of a theory of dispersion relationships in reflection.

Additional information on energy band edges has been obtained from Hall effect and piezoresistance studies. Studies of surface transport phenomena in semiconductors received clarification from a reformulation of the Boltzmann equation to treat both weak and strong fields. Field effects studies of epitaxially grown crystal films of PbS are expected to add to our understanding of photoconductivity in these materials.

Research on the fundamental nature of magnetic materials has been directed toward understanding magneto-elastic interactions, distribution of charge density of unpaired electrons in the transition metals, magnetic properties of compounds of $PrCo_5$ and $NdCo_5$, and changes in the crystal lattice occurring at the Curie temperature. Certain aspects of the magnetic material research have been concerned with development of magnetic alloys resistant to extreme environments such as high temperature and particle irradiation that may be encountered in outer space or in the vicinity of nuclear reactors. A fundamental study of Barkhausen noise and its relation to magnetometry noise was also begun on various high permeability magnetic materials.

Accurate measurements of the elastic constants for single crystals of yttrium iron garnet were made which have helped to clarify the phenomena of magnetostriction and magnetoacoustic interactions.

Theoretical studies on the potential energy of the Si-O-Si bond in SiO_2 have investigated an anomaly observed in the relationship between specific heat and temperature dependence of the elastic moduli of SiO_2 glass.

Studies of the light pattern of laser crystals by means of ultra-high speed camera techniques have revealed interesting insight into the mechanism of light output from lasers.

Investigations of intermetallic compounds have led to the development of a series of unique alloys based on a compound of nickel and titanium (TiNi) and related phases (Ti_2Ni) and ($TiNi_3$). These alloys have a potential for many applications where a combination of hardness, non-magnetic, corrosion and abrasion resistance properties are required.

In the area of electromagnetic devices, a low power drain magnetometer utilizing a ring magnetic core sensor has found application in space vehicles for determining its attitude with respect to the earth's magnetic field.

Concerning microwave devices, the development of suitable sphere grinding and polishing techniques and an improved line-width measurement technique represents the solution of the major production problems associated with the development of practical cavity ferromagnetic masers.

Table I lists a resume of the more important accomplishments of the Department for the year 1961 arranged according to their contributions to basic concepts and also an indication as to how these results will lead to improvement in the military Navy program.

TABLE I

RESUME OF ACCOMPLISHMENTS (1961)

Areas of Investigation	Important Results	Increases our Basic Understanding of	Which leads to Improvements in
Electrical Properties of PbTe	Measurements extended to very high carrier concentrations	Band structure and scattering mechanisms	Model for lead salt properties
Free-Carrier Absorption of PbTe	Dependence on wave-length determined; extra absorption found	Scattering mechanisms; energy-band structure	Improved model for lead salt properties
Reflectivity of PbTe	Effective mass varies strongly with carrier concentration	Band structure of lead salts	Improved model for lead salt properties
PbTe etch	Highly polished surfaces prepared which allow improved reflectivity measurements	Etching and surface phenomena	Surface treatment of electrical and photosensitive devices
Tin Telluride Single Crystals	Very high carrier concentrations achieved	Deviations from stoichiometry	

TABLE I (CONT'D)

Areas of Investigation	Important Results	Increases our Basic Understanding of	Which leads to Improvements in
Surface Transport in Lead Salts	Dependence of surface thermoelectric power on surface potential	Transport mechanism	Improved model for lead salt properties
Epitaxial Growth Lead Salts	Mobilities approach those of bulk PbS	Scattering mechanisms; photo-effects; structure of films	Infrared detectors
Surface Studies of PbS	Frequency dependence of field effect	Relation of surface trapping to photoconductivity recombination	Infrared detectors
Reflectivity and Optical Properties of InAs, InSb, GaAs	Optical constants determined in visible and near-ultraviolet	Band structure in a range not otherwise accessible	Semiconductor devices
Laser Mechanisms	Emission pattern rapidly changing with time	Excitation threshold mechanism	Optical ranging and communication devices
Thermal Coefficient of Expansion of Lead and Tin Salts	Expansion coefficients determined from X-ray lattice parameters	Thermodynamic properties	Quantitative calculations requiring accurate lattice constants
Magneto-Elastic Coupling	Relation of magnetization to temperature dependence of magnetostriction coefficients	Understanding of magnetoelastic coupling	
Rare Earth Compounds	$PrCo_5$ and $NdCo_5$ prepared to determine moment	Antiparallel moment alignment	Inductors and motors

TABLE I (CONT'D)

Areas of Investigation	Important Results	Increases our Basic Understanding of	Which leads to Improvements in
Neutron Diffraction	Aspherical charge distribution in iron Localized moments in $FePd_3$, $CrPt_3$, $MnPt_3$, spin densities in Mn_2Sb	Magnetic structure	Magnetic materials
Ferrite Substitutions	Zinc for lithium substitution increases moment and reduces Curie point	Particular exchange coefficients	Special purpose materials
Gadolinium-Manganese Compounds	Structure determination of $GdMn_6$	Spin behavior	High induction magnetic material
Magnetic Noise	Instrumentation to determine fluctuations of intrinsic magnetization	Magnetic switching resonance damping	Magnetometers-High frequency, low loss memories
Barkhausen Noise (Magnetic Core)	Apparatus for measuring core noise in highest permeability materials	Effects of core material and structure on flux-gate magnetometer self noise	Magnetometers
Magnetic Alloys	Environmental resistant alloys	Structure and ferromagnetism	Magnetic devices operating at high temp. and radiation levels
Very High Pressures (Magnetic materials)	Facility for 70,000 atm at high temperature-Produced synthetic diamonds	Metal structure	Magnetic and non-magnetic materials
Intermetallic Compounds	Important engineering alloys based on TiNi	Intermetallic structures	Engineering alloys

TABLE I (CONT'D)

Areas of Investigation	Important Results	Increases our Basic Understanding of	Which leads to Improvements in
Ferromagnetic Line Width	Improved measurement technique	Spin wave losses	Ferromagnetic masers
Flux-Gate Magnetometry	New ring core sensor	Ferromagnetic circuitry	Low-power drain Magnetometers
Magnetic Amplifiers	Ultra-stable high-gain circuits	Limiting noise processes	Low-signal level amplifiers
Non-Linear Circuitry	New principle of detection	Operation of modulator and magnetometer circuits	Modulation detectors
Elastic Properties of SiO_2	Extended Si-O-Si bond explains specific heat anomaly	Structure of amorphous solids	Dielectrics and refractories
Acoustic Impedance of Indium	1-10 KMC acoustic transmission characteristics	Specific heat	Superconducting devices
Particle Radiation Effects (Magnetic Materials)	Magnetic properties changed drastically by proton irradiation	Influence of defects on magnetic properties	Magnetic materials

PROPERTIES OF LEAD TELLURIDE

The Phase Diagram of Lead Telluride

Lead telluride is a compound semiconductor composed of two volatile components. Therefore, in order to determine its phase diagram completely, the temperature-composition and temperature-pressure projections must be specified.

Using the technique previously reported to determine the temperature-pressure projection (see Figure 1) and the results as previously reported for the temperature-composition projection, the three-phase line has been determined at the tellurium rich limit of stability. The internal structure, Schottky constant, lead-rich limit of stability, and intrinsic partial pressure, were calculated from a theory for the limits of stability of a binary semiconductor. The Schottky constant and the internal structure were sensitive to the choice of intrinsic carrier concentration, whereas the activation energy of the Schottky constant and the intrinsic partial pressure were fairly insensitive.

Valence Bands in PbTe

Earlier we reported that the magnetoresistance symmetry in p-type PbTe is consistent with <111> - valleys in the valence band. De Haas-van Alphen oscillations in the magnetic susceptibility of p-type PbTe at 4.2°K have been observed at the University of Pennsylvania, using our crystals. These observations have indicated the presence of another energy surface, one which is approximately spherical in form.

We have studied the Hall coefficient in p-type PbTe at 77°K as a function of magnetic field intensity and carrier concentration in an attempt to detect the usual two-band effects. These effects were not found. From their absence we can only conclude that the carrier mobilities in the spherical energy surface and in the ellipsoids must be nearly the same, and that the energy difference between the band edges of the two types of surfaces must be small. The latter conclusion has since been verified by further study of the de Haas-van Alphen effect.

A study was made of the "anomalous" increase in the Hall coefficient between 77°K and room temperature in p-type PbTe. The ratio of the room temperature value to that of 77°K is about 1.2 for a carrier concentration of 5×10^{17} per cm^3, and steadily increases to a value of 2.2 at 1.3×10^{20} carriers per cm^3. We originally believed that this behavior was due to the transfer of carriers into another valence band located roughly 0.1 ev below the ellipsoidal band edge, but the persistence of the effect to such high carrier concentrations makes this explanation less likely. An alternative explanation is that the effect results from the non-parabolic nature of the valence band.

Piezoresistance of PbTe

Piezoresistance coefficients relate fractional changes in resistivity of a material to applied stress. These coefficients are in turn related to elastoresistance coefficients through the elastic stiffness constants.

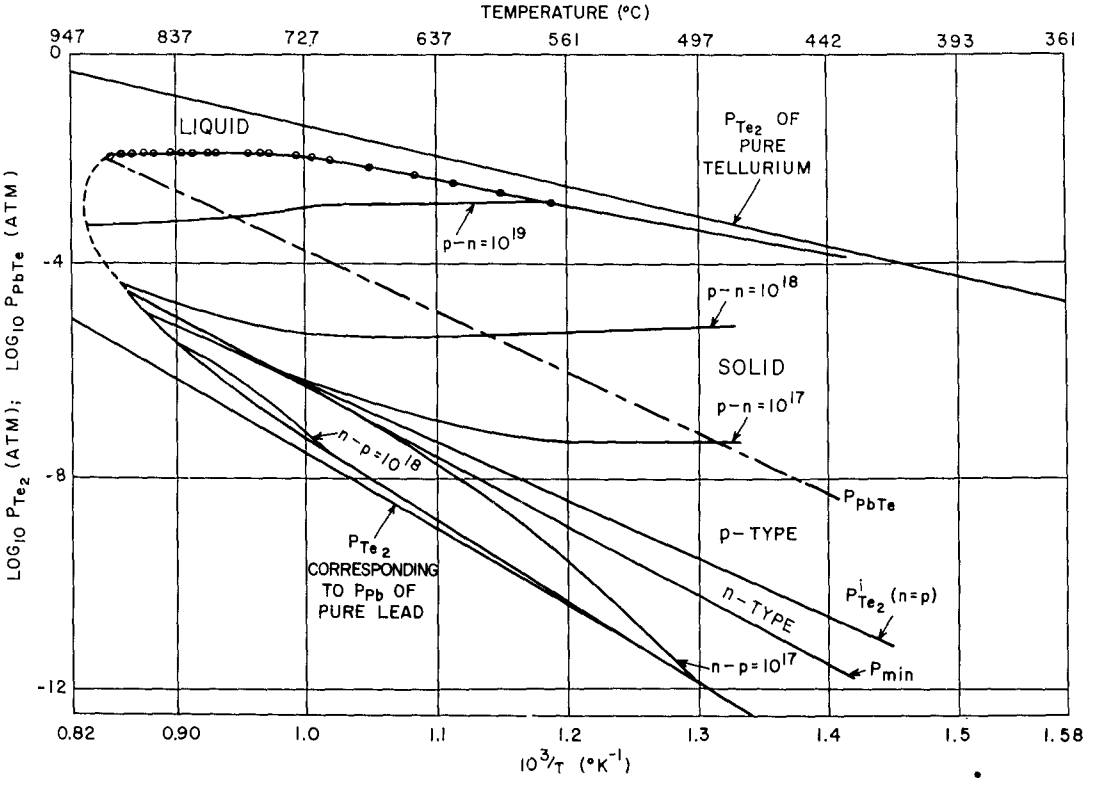

Fig. 1 Temperature dependence of the partial pressure of diatomic tellurium at the three-phase limit (solid and dotted curve), partial pressure of lead telluride (P_{PbTe}), internal structure (n-p or p-n = 10^{18} etc.), sublimation line ($P_{min.}$), and the intrinsic partial pressure ($P^i_{Te_2}$).

Room temperature measurements have been made on pulled single crystals of p-type PbTe with about 3×10^{18} holes/cm^3. The piezoresistance coefficients were determined from the application of uniaxial stresses and hydrostatic pressure. We found that π_{11}, π_{12}, and π_{44} equalled 24, 15, and 215 x 10^{-12}cm^2/dyne for uniaxial stress up to 10^8 dynes/cm^2 and hydrostatic pressure up to 1800 atmospheres. From acoustical measurements it was found that $1/3\ (C_{11} + 2C_{12})$, $1/2\ (C_{11} - C_{12})$, and C_{44} equalled 4.16, 4.90, and 1.31×10^{11} dynes/cm^2. The elastoresistance values for $1/3\ (m_{11} + m_{12})$, $1/2\ (m_{11} - m_{12})$, and m_{44} of 23, 4.4, and 28, respectively, were then computed. These results suggest a <111> - multivalley model for the valence band of PbTe. However, the pressure coefficient $1/3\ (m_{11} + 2m_{12})$ is very large for an extrinsic material and indicates the possibility of another valence band or a strain dependence of the effective mass.

We also measured the pressure coefficient of an n-type sample of PbTe with about 9×10^{17} electrons/cm^3. Up to 1800 atmospheres $1/3\ (m_{11} + 2m_{12}) = 20$.

Reflectivity of P-Type Lead Telluride in the Infrared Region

Free carriers in a semiconductor can produce large variations in the reflectivity in the infrared region when the carrier concentration is large. The corresponding variations in the optical constants can be analyzed to give valuable information regarding the effective masses and scattering mechanisms associated with the free carriers.

The reflectivities at near-normal incidence of p-type PbTe having hole concentrations varying from 3.0×10^{18} to 4.6×10^{19} cm^{-3}, have been measured in the spectral range from 3 to 32 microns. A typical reflectivity curve is shown in Figure 2 along with the corresponding variations in the index of refraction, n, and extinction coefficient, k. Both n and k were determined by applying the Kramers-Kronig dispersion relation to the reflectivity data. The distinct dip in the reflectivity at approximately 12 microns is due to the contribution of free carriers to the electric susceptibility. An analysis of the data gives values of the susceptibility effective mass, m_S, which increases with the carrier concentration. At hole concentrations of 3.0×10^{18} and 4.6×10^{19} cm^{-3}, m_S was found to be 0.11 ± 0.02 and $0.20 \pm 0.02\ m_o$, respectively, where m_o is the rest mass of the free electrons. Free carrier scattering times have also been determined from the reflectivity data and are in reasonable agreement with the scattering times calculated from carrier mobilities.

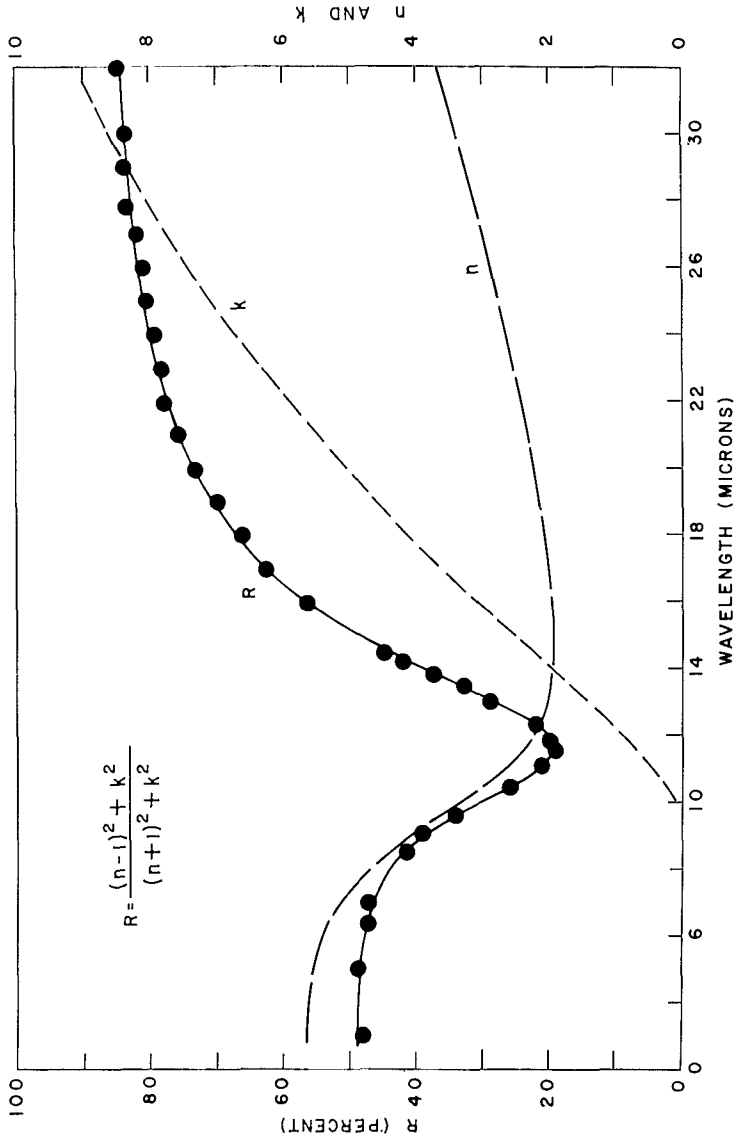

Fig. 2 Reflectivity of p-Type PbTe having a hole concentration of 4.6×10^{19} cm^{-3}. The index of refraction, and extinction coefficient, k, also are given.

Free Carrier Absorption in p-Type PbTe

The transmission of infrared radiation through a semiconductor can give valuable information about the band structure and carrier scattering mechanisms. Often, within a relatively short region of the transmitted spectrum, it is possible to observe absorption which is due to a variety of absorption mechanisms.

Infrared absorption measurements have been made on p-type PbTe having carrier concentrations ranging from 4.97×10^{17} cm^{-3} to 6.99×10^{18} cm^{-3} and at temperatures between 300°K and 77°K. A typical absorption spectrum is shown in Figure 3. In region A, the steep rise in the absorption coefficient is the fundamental absorption edge - which indicates that the width of the forbidden energy gap is 0.3 ev. In region C, the absorption is dominated by the classical free carrier effect. The expression for this type of absorption is

$$\alpha = \text{Const.} \frac{N\lambda^2}{n\mu \left(\frac{m^*}{m} \right)^2} \qquad (1)$$

where N is the free carrier density, λ is the wavelength, n is the index of refraction at wavelength λ, μ is the carrier mobility, and $\left(\frac{m^*}{m}\right)$ is the effective mass of free carriers. Experimentally determined wavelength dependence of α is in good agreement with equation (1). It is found that α is proportional to the 2.0 ± 0.2 power of λ for all temperatures and carrier concentrations for which this type of absorption could be measured. The magnitude of α calculated using values of μ and $\left(\frac{m^*}{m}\right)$ determined from other experiments is also in good agreement with the experimental data. In region B, the absorption is due to a combination of the classical free carrier absorption and an additional absorption band. The magnitude of this additional absorption is proportional to the carrier concentration and decreases as the temperature is lowered. The explanation of the additional absorption will serve as a critical test for proposed band structure models.

An Electrolytic Polish and Etch for Lead Telluride

A need had arisen for an electrolytic polish that would produce surfaces satisfactory for reflectivity measurements. In addition, because the polishing had to be carried out at 90-105°C, the crystals should be free of cracks by thermal shock. These cracks were preferentially attacked during produced electropolishing.

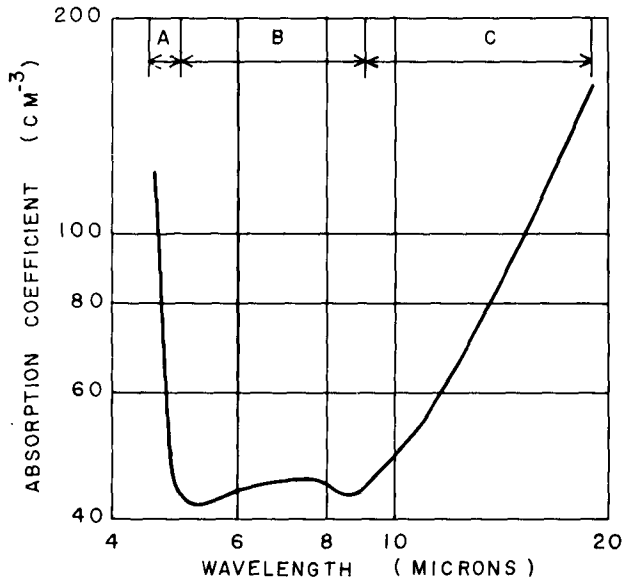

Fig. 3 The absorption coefficient vs wavelength for a p-type sample at 190°K with carrier concentration equal to 9.06×10^{17} cm^{-3}.

An electropolishing procedure has been developed that gives a smooth, shiny surface on single-phase, p-type lead telluride, both on single crystals and on polycrystalline material. This procedure produced a surface that was satisfactory for reflectivity measurements because it removed the worked layer left by grinding and polishing, leaving a smooth surface free of residual film. An electrolyte containing potassium hydroxide, water, glycerol, and ethanol was used. The piece of lead telluride to be polished serves as the anode and a piece of platinum foil as the cathode. By lowering the voltage across the cell, the electropolishing procedure was used for electroetching. Etch pits were formed on p-type lead telluride (both on single crystals and on polycrystalline material). They were formed only on surfaces approximately parallel to the cleavage surfaces. The pits were generally square and pyramidal and about 5-10μ across. They occurred along small-angle grain boundaries, traces of active slip planes, and at random points on the surface. Crystals deformed plastically and etched before and immediately after the deformation showed pits that appeared to be due to dislocations introduced by the deformation.

TIN TELLURIDE

Preparation of Tin Telluride Single Crystals

Tin telluride is similar to the lead compound semiconductors. It has the same lattice structure as the lead compounds. The limited information on tin telluride available in the literature indicated that considerable insight into the nature of SnTe could be gained from a systematic study similar to the one carried out at NOL on PbTe.

High quality SnTe single crystals were grown by using the Czochralski technique and the apparatus developed for growing PbTe crystals. The stoichiometry of the SnTe crystals was varied over a wide range by means of a technique developed for PbTe, which brings small crystals to a composition limit of stability at the temperature which the treatment is to be carried out. Information obtained from these studies indicates that SnTe has a much wider composition range of stability than any of the lead compound semiconductors and that the range lies entirely on the tellurium rich side of the stoichiometric composition. The range is so wide that it can be measured by ordinary methods of chemical analysis. Chemical analysis indicates that the composition limits at 600°C are at 50.1 atomic percent Te and 51.4 atomic percent Te. The crystals as pulled from a stoichiometric melt are 50.6 atomic percent Te. Such large deviations from stoichiometry imply large concentrations of defects, concentrations that are a few percent of the concentration of normal lattice sites. Such large concentrations produce easily measurable changes in the lattice parameters and densities of the crystals which can give direct information about the nature of the defects. As would be expected by analogy with PbTe, these crystals are all p-type with large carrier concentrations.

Electrical Properties of Tin Telluride

The Hall coefficient R and the resistivity ρ between room temperature and 4.2°K for three representative samples of SnTe single crystals is shown in Figure 4. The Hall coefficients, which on a one-carrier basis correspond to carrier concentrations between 1.4 and 17 x 10^{20} holes/cm^3, are constant below about 150°K, but rise gradually at higher temperatures. This effect, which is also observed in p-type PbTe, may result from the presence of more than one valence band, or from nonparabolic bands.

The room temperature resistivity is practically independent of carrier concentration over the range studies; as the temperature is lowered, the resistivity decreases to a limiting "residual resistance," the value of which increases rapidly with increasing carrier concentration. This resistivity behavior may be explained qualitatively by a combination of temperature-dependent acoustical lattice scattering and temperature-independent point-defect scattering, taking into account the effect of degenerate statistics on both. Hall mobilities calculated from the Hall and resistivity data for some twenty samples investigated are smoothly varying functions of carrier concentration, and suggest a high degree of sample homogeneity. Mobility values at room temperature, 77°K, and 4.2°K for the three typical crystals of Figure 4 are summarized in Table II.

TABLE II

HALL MOBILITIES IN p-TYPE SnTe

Sample No.	Carrier Concentration	Hall Mobility (cm^2/v-sec) 298°K	77°K	4.2°K
1	1.40 x $10^{20}/cm^3$	517	1460	4540
2	7.72	80.2	191	298
3	17.4	37.7	75.5	96.7

SURFACE EFFECTS

Surface Studies on Chemically Deposited PbS Photocells

PbS photocells were one of the earliest infrared detectors used. Their high signal to noise character and high impedance have made them the most commonly used detector in the 1-3μ wavelength region. Despite their widespread use, the mechanism of photosensitivity is still obscure. For a number of years surface properties of these cells have been studied by means of the frequency dependences of the field effect. It has long been known that the properties of the films are strongly dependent on the charac-

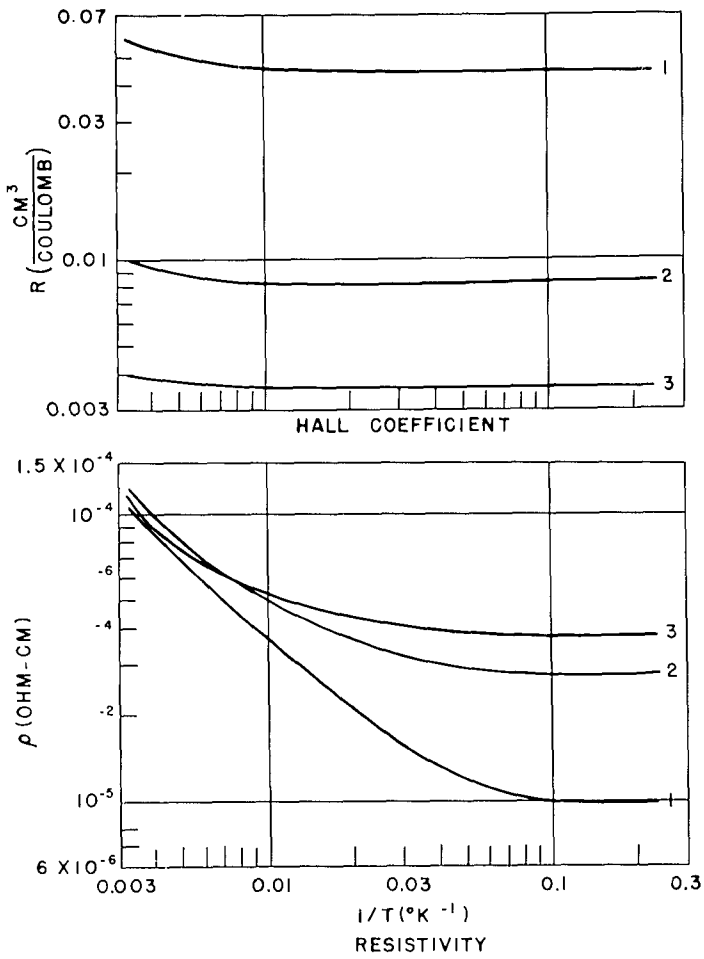

Fig. 4 Hall coefficient and resistivity vs temperature in p-type SnTe samples of Table II.

ter of the surface treatment. These field effect measurements have shown that the surface trapping states and photoconductive recombination centers are very closely related. By combining surface and photoconductive measurements, additional understanding of the photoconductive mechanism may be reached.

In the past year, an apparatus has been completed which measures the frequency dependence of the field effect in a semiautomatic fashion. Presently, the apparatus is capable of examining the frequency range from 10 cycles to 20 kc. A minor modification will enable us to extend the frequency range to 50 kc when necessary. The temperature dependence of the field effect on PbS will be continued and the temperature range extended -85°C to + 150°C. Preliminary studies of PbSe photocells are also being conducted in cooperation with the Santa Barbara Research Center.

Preparation and Properties of Epitaxially Grown PbS Films

Epitaxy is the process of orienting a deposited layer by the crystalline character of the substrate. This phenomenon has become widely used in the production of semiconductor devices such as diodes, transistors, and heterojunctions. Despite the large scale use of epitaxially grown layers very little is known about their electrical properties.

In this study a number of PbS films were prepared by vapor deposition on cleaved rock salt surfaces. These films showed a high degree of orientation as determined by the cracks in the film. The carrier concentration was in the $10^{18}/cm^3$ range and was essentially independent of temperature. While the mobility showed a dependence on temperature reminiscent of the $T^{-5}/^2$ bulk dependence at high temperatures, it leveled off quite rapidly as the temperature decreased. The films are quite different in these respects from the photosensitive PbS films by either chemical or vapor deposition. Further work is being done to define more precisely the properties of these epitaxial films.

Surface Transport

Much of our knowledge of the structure and physics of semiconductor surfaces comes from the study of electronic transport processes in the surface space charge region (SSCR). By making both measurements and theoretical predictions of various thermoelectric and galvanomagnetic effects in the SSCR, the present program is concerned with how the band structure and transport mechanisms in the SSCR differ from those in the bulk.

The Boltzmann equation theory of surface thermoelectric effects has been reformulated to include strong as well as weak SSCR fields. Calculations have been carried out on the IBM 704 computer for strongly intrinsic Germanium at 77°K for both specular and diffuse surface scattering conditions. The calculations predict that the dependence of surface thermoelectric power on surface potential will show cuspoidal behavior in the

diffuse but not in the specular case. A measurement of this dependence might then permit us to decide which condition actually occurs in nature.

A vacuum cryostat has been constructed and put into operation providing stable temperatures between 100°K and 300°K that are required for the measurement of surface thermoelectric and galvanomagnetic effects as a function of the SSCR potential. This potential was varied by means of transverse field electrodes insulated by $BaTiO_3$ spacers 20-50 micron thick. Preliminary measurements at 100°K of the Hall effect with a 10^{11} - 10^{12} imp/cm^3 sample are in reasonable agreement with the earlier work at 196°K on similar material.

Recombination Lifetime in Indium Antimonide

The study of the mechanism of carrier recombination in indium antimonide has been continued in an effort to understand more completely the lifetime of intermetallic semiconductors, which limits the performance of many electrical and optical devices.

The experimental arrangement and techniques for measuring carrier recombination lifetimes were completed and methods for controlling the effects of surface recombination were perfected. Measurements were made of the change in sample resistance and photoconductivity while a surface field was applied to the indium antimonide. Preliminary results have evaluated the surface potential for both n and p-type samples. These results have given a value for the surface mobility of holes on p-type material (u_S = 638) and for electrons on n-type material (u_S = 475). They also have given a surface state density greater than 6 x 10^{11}cm^{-2}. This value is much larger than the values obtained by other workers on germanium, however, it would explain the shielding of the surface space charge layer from the surface field which we see in these experiments. Better methods of measuring the surface properties are expected to produce an understanding of the surface recombination centers.

LEAD SELENIDE COMPOSITION STABILITY LIMITS

Lead selenide is a compound semiconductor that exists over a narrow range of composition. To determine the solidus lines, the same technique as previously reported for lead telluride was used. Pb-saturated and Se-saturated PbSe were prepared by equilibrating small crystals with two-phase ingots rich in either Pb or Se. These crystals were then quenched to room temperature. The Hall constant and the conductivity were then measured.

Pb-saturated PbSe was found to be n-type with a room temperature electron concentration that increased with increasing equilibration temperature from about 1.7 x 10^{18}cm^{-3} at 500°C to 1.4 x 10^{19}cm^{-3} at 800°C. (See Table III). The carrier concentrations were independent of quench rate in the range used and were proportional to exp (-E/kt) with E = 0.49 ev. Selenium-saturated PbSe was found to be p-type, the room temperature hole

concentration definitely depending on the quench rates used at 600°C and above. (See Table IV). The hole concentrations are between 3 and 6.5 x 10^{18} cm^{-3}. Near 600°C PbSe exists as a stable phase over a composition range whose limits are roughly symmetric about the stoichiometric composition and which is at least 0.012 atomic percent wide.

TABLE III

EQUILIBRATION TIMES AND TEMPERATURES, AND ROOM TEMPERATURE ELECTRON CONCENTRATION FOR Pb-SATURATED PbSe

Run	T(°C)	Time (Hours)	Electron Concentration x 10^{-18}
1	805	51	12.0, 13.6
2	706	92	8.62, 8.01
3	590	170	3.85, 3.32
4	800	48	14.4, 11.6
5	500	403	1.64, 1.75

TABLE IV

EQUILIBRATION TEMPERATURES AND TIMES, AND ROOM TEMPERATURE HOLE CONCENTRATIONS FOR Se-SATURATED PbSe

Run	T (°C)	Time (Hours)	Hole Concentration x 10^{-18}
1	706	92	4.62
2	590	170	4.71, 5.32
3	584	168	6.67, 6.08
4	504	92	2.94, 3.00

OPTICAL STUDIES

Dispersion Relation for Reflectivity

The optical properties of a material can be measured readily in regions of the spectrum where the material transmits electromagnetic radiation. But when the material becomes so opaque that transmission measurements are no longer possible, one must rely on reflectivity measurements alone. One conventional way to deduce optical constants is to study the reflectivity using polarized light at non-normal incidence. Two measurements are required to determine the index of refraction n and the extinction coefficient k, and a tedious numerical procedure is required since the measured quantities depend in a complicated way on the optical constants.

In the last few years a new method has been used for studying optical properties which requires only a single measurement, usually the reflectivity at normal incidence, at each wavelength. As a consequence of the requirement, called the causality requirement, that an effect cannot precede the cause, there is a relation between the phase shift on reflection and the magnitude of the reflectivity itself. This dispersion relation can be used to calculate the phase shift if the reflectivity is known over a wide enough range of photon wavelengths. The optical constants are then easily calculated from the phase shift and the reflectivity. This method has been successfully used at the Naval Ordnance Laboratory to study the optical constants of semiconductors in the visible and ultraviolet parts of the spectrum, where intrinsic properties are dominant, and in the infrared, where free-carrier effects can be studied.

Reflectivity and Optical Constants of Intermetallic Semiconductors

As described above, it is possible to determine the optical properties of a material from reflectivity data taken at a single incident angle over a large frequency range if a dispersion relation is used between the phase and the magnitude of the reflectivity. The optical constants in the visible and ultraviolet regions of the spectrum give information about major features of the electronic energy band structure, far from the ordinarily observed energy gap, which are difficult to study experimentally in any other way.

The reflectivities of indium arsenide, indium antimonide, and gallium arsenide were measured at normal incidence from 2050 A to 15u at room temperature. Various mechanical polishing techniques and chemical etches were employed to study the variation in overall magnitude and in structural detail of the reflectivity as a function of wavelength. The reflectivities obtained show peaks near 2.5 and 5.0 ev, with splitting of the lower maximum into two smaller peaks whose separations are 0.35, 0.50, and 0.20 ev, respectively for the three compounds studied. Figure 5 shows experimental reflectivity data obtained from two different mechanical polishes of an indium antimonide sample. From the best reflectivity data of each material, the optical constants were computed in the range 0-6.0 ev, and these results are shown in Figure 6 where n and k are the real and imaginary parts of the

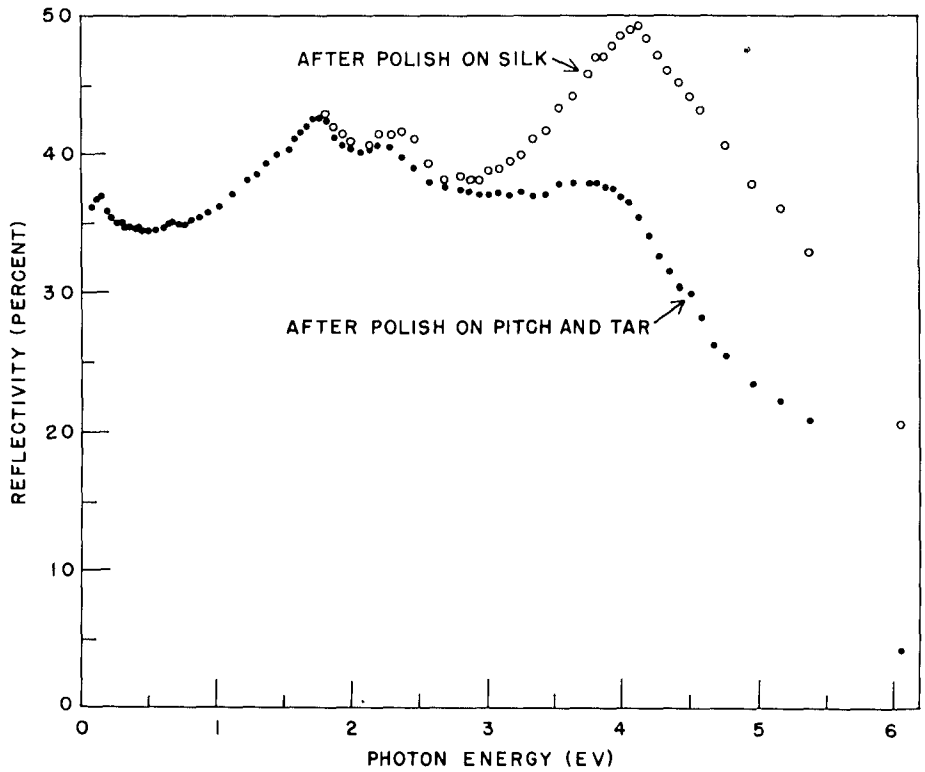

Fig. 5 Reflectivity of Indium Antimonide Sample for two different surface polishes.

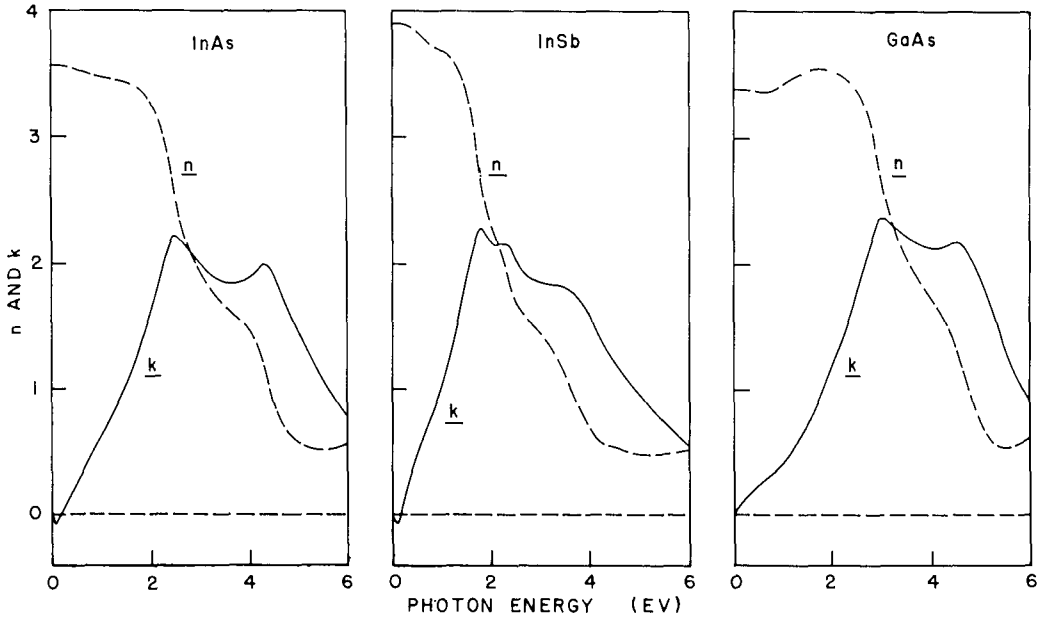

Fig. 6 Calculated values of the Optical Constants, $\underline{n}$ and $\underline{k}$, from reflectivity data for Indium Arsenide, Indium Antimonide, and Gallium Arsenide.

refractive index. The imaginary part of the reciprocal of the dielectric constant for each of these materials appears to have a maximum somewhat beyond 6.0 ev. Photons of that energy would be strongly excited by fast charged particles.

LASER MECHANISMS

Operating laser devices are known to produce a series of somewhat erratic light pulses with a duration of one microsecond or less. The spreading angle of the resulting light beam has proven to be much greater than was at first anticipated. The internal mechanism associated with the transfer of energy from the pumping light to the emitted beam seems to be much more complicated than was originally supposed.

Extremely high-speed photography was used to determine the phenomena associated with individual pulses of light. NOL is using its shock-tube photographic equipment to make such studies. A ruby laser, one of the first put into operation by the Navy, was constructed and high-speed photographs of the emitting surface were taken. The emission pattern shows definite geometrical structure in some cases (see cover illustration). The pattern was found to change in time of the order of one microsecond. Although the nature of the laser phenomena is not understood in adequate detail as yet, it seems this photographic method can produce experimental data of value in explaining the basic mechanisms involved.

MAGNETIC SPIN-LATTICE PROPERTIES

Magnetoelastic Coupling Interaction

Magnetoelastic coupling, the source of magnetostriction, alters the temperature dependence of magnetocrystalline anisotropy, contributes to the specific heat and ultrasonic absorption, and affects the ferromagnetic resonance line width and loss.

A very general theory, first order in the strains but up to sixth order in the magnetization direction cosines has been developed. This theory relates the temperature dependence of the magnetostriction coefficients to those of the magnetization and enables one to calculate the specific heat and magnetic anisotropy terms.

The experimental arrangement is nearing completion for measurements of the magnetoelastic coupling coefficients that occur in the theory as phenomonological parameters.

Aspherical Charge Distributions in Transition Metals

One of the results of using the powerful neutron-diffraction method for studying magnetic structures of solids has been the quantitative determination of the spatial distribution of the charge density of unpaired electrons. Particularly interesting has been the discovery that the charge distribution deviates from spherical symmetry. This result is not surprising, since the atom in a crystal has a non-spherical environment. The asphericity observed in non-metals has been satisfactorily accounted for in many cases, but the results for metals could not be analyzed on the basis of the existing theory.

A theory of the asphericity of the charge distribution in cubic metals was formulated and used to calculate the effect in body-centered cubic iron. The theoretically predicted asphericity for iron was found to be in good agreement with experimental results. Some cruder estimates for cobalt and nickel were also consistent with experimental results. The theory was used to estimate the asphericity that would be determined from the coherent scattering by several ferromagnetic body-centered cubic alloys.

Spin Densities in Transition Metal Atoms

Considerable effort has been expended in determining the amount of information about the unpaired electron distribution that can be reliably derived from Fourier inversion of magnetic form factors such as those of Fe_3Al and NiO, which were described in last year's report. Termination of the Fourier series at limiting scattering angles that are available in the laboratory still leaves considerable resolvable detail in projections of the spin density. We have found that the form factor of an antiferromagnet can be put on an absolute scale, without knowledge of the spin per atom, by integrating the charge density around each atom, so long as the atoms are resolved. These investigations establish spin density mapping as an important tool in investigating the electronic structure of magnetic atoms. Typical two-dimensional projections obtained from such data are illustrated in Figures 7 and 8.

The spin densities in the intermetallic ferrimagnetic compound Mn_2Sb were studied by the polarized neutron method and by Fourier projections. Enough data have already been collected to show that the two types of manganese atom in this lattice have different radial spin densities and also that both are anisotropic.

Change in Lattice Constant at Curie Temperature

One of the problems in antiferromagnetism has been the relation of the spin ordering and direction in the magnetic lattice and the lattice distortions that accompany this ordering process. Early work of others explained the distortions at the transition temperature in terms of the exchange integral. For certain oxides other effects must also be considered.

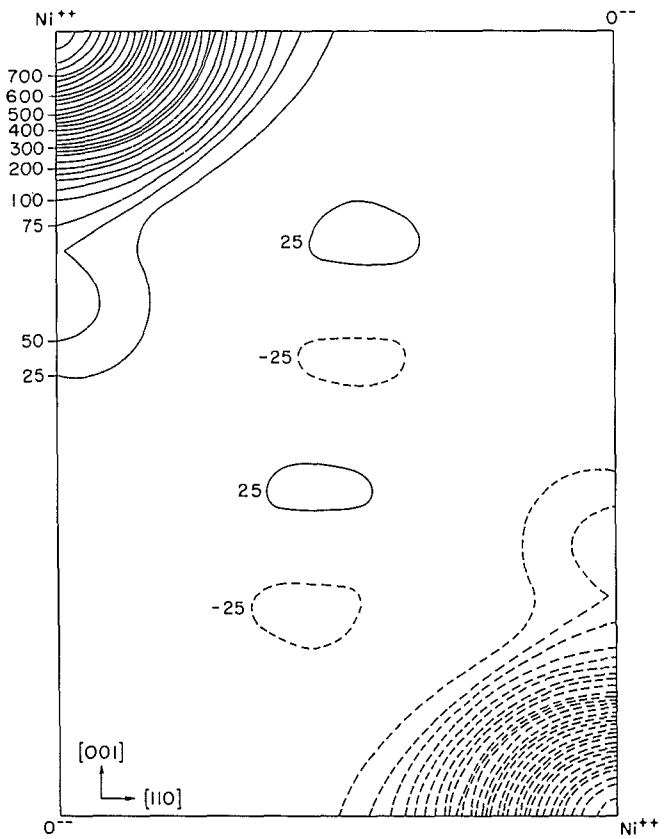

Fig. 7 A projection of the spin density in NiO on the $(1\bar{1}0)$ plane. (Solid lines represent positive density, dashed lines, negative, with arbitrary units.) Note the elongation of the electron density along the $[001]$ and the projected $[010]$, $[100]$ axes, characteristic of e_g symmetry. The negative density is a consequence of the antiferromagnetic alignment of Ni^{++} spins.

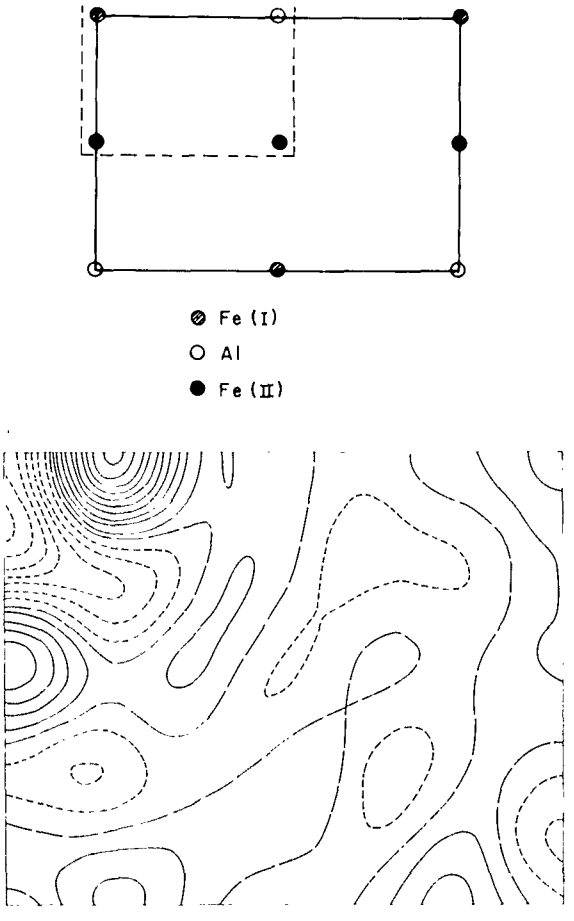

Fig. 8 A projection of Fe_3Al, also on (110), but here the equivalent spherical density has been subtracted. Hence the e_g-like symmetry of the Fe (I) atom (which has only Fe near neighbors) appears as an excess of charge along the cube edges and a deficiency along the cube diagonal. Contours here are plotted at intervals of 0.063 Bohr magnetons per square angstrom. The upper diagram locates the atoms and the area covered by the projection.

Using a back reflection Debye powder camera, X-ray photographs were taken of MnO_2 and MnF_2 to determine the behavior of the lattice constants near the transition temperature. It was found that on lowering the temperature, the c-axis of MnO_2 expands while that of MnF_2 contracts. Results for MnO_2 and MnF_2 as well as other antiferromagnetics, show that, within a given crystal structure, there is a correlation between the distortion and the spin direction.

Magnetic Noise Measurements

Magnetization fluctuations responsible for magnetic noise arise from two essentially different processes: Domain wall motion and fluctuations of the magnetization within the domain. The analysis is expected to yield information regarding the interaction of domain walls containing impurities. Fluctuations of intrinsic magnetization are analogous to Johnson type voltage fluctuations in electrical circuits. Analysis of measurements provides a possible method for studying the spin-lattice interaction.

It is expected that magnetic noise measurements will provide a method of investigating fundamental properties of ferro- and ferri-magnetic materials. The construction of the experimental apparatus is essentially complete.

Determination of Magnetic Structures

Neutron diffraction measurements on polycrystalline specimens have been used to gather information about spin alignment and atomic positions in several spinel and alloy systems.

The previously reported Yafet-Kittel triangular spin arrangement in $CuCr_2O_4$ was confirmed by measurements at low temperatures utilizing an applied magnetic field. It was found that the magnetic scattering for certain reflections increased when the field was applied, by an amount accurately predicted by the model. The cation distribution in the mixed series $Mn_xFe_{3-x}O_4$ was determined for compositions on either side of the point ($x \sim 0.6$) at which an anomaly in the magnetic anisotropy was observed. Results indicate that the percentage of Mn^{2+} ions on tetrahedral sites remains roughly constant at $\sim 80\%$ for $0<x<1$. Any abrupt change in this parameter is therefore ruled out as the origin of the anisotropy behavior.

Investigation of alloys of elements of the first transition series with Pd and Pt was conducted to confirm the suggestion, based on magnetization measurements, that a localized moment is induced on the normally non-magnetic atoms. Measurement of the ordered structures $FePd_3$, $CrPt_3$, and $MnPt_3$ has verified the existence of localized moments on both the Pd and Pt atoms. Moreover, the alignment in $CrPt_3$ was found to be ferrimagnetic, so that apparently the sign as well as the magnitude of the interaction between the first and higher transition series element varies with position in the periodic table.

Theoretical Model of Ferromagnetic Relaxation

A theoretical model of ferromagnetic relaxation has been developed to describe the dispersion of initial permeability. This model quantitatively describes the behavior of the complex initial permeability as a function of frequency using two parameters, the DC initial permeability and a viscosity coefficient. Some of the simple results of the analysis show that:

1. The model can be derived from the Landau-Lifshitz equation of motion.

2. The phenomenon is mainly one of dispersion as contrasted to one of resonance.

3. At the dispersion frequency both the real and imaginary parts of the complex permeability are approximately equal to half of the DC initial permeability.

4. The limiting frequency of a material is approximately equal to the dispersion frequency times the initial permeability.

The analysis has been extended to include calculations of curves which enable one to estimate the percent error encountered in measuring the complex permeability at the dispersion frequency.

MAGNETIZATION OF RARE EARTH ALLOYS

Magnetism in Praseodymium and Neodymium-Cobalt Compounds

Most of the rare earths, form with cobalt, an intermetallic compound of stoichiometry given by the formula (rare earth) Co_5. The magnitude of the spontaneous magnetic moments of these compounds indicates that the rare earth moment is participating in the cooperative magnetism. The saturation moment can be well accounted for in most instances by assuming that the rare earth moment is aligned anti-parallel to the five cobalt moments and that the moments of the atoms are the same in the compounds as in the pure metals. Two exceptions seem to be the compounds in which the rare earth is either praseodymium or neodymium. These have been reported to exhibit a higher saturation moment than calculated for a strictly antiparallel alignment. An argument based on the way in which the ground state total angular momentum of the rare earth ion is compounded from spin and orbital angular momenta leads one to believe that a parallel alignment of rare earth and cobalt moments is reasonable in these two compounds.

To test this hypothesis, the compounds $PrCo_5$ and $NdCo_5$ were prepared. Although X-ray diffraction indicated a single phase of the correct structure, in each case, the saturation moments observed were not quite as large as those reported by others. This difference is believed to be due either to inadequate saturation of the material or to undetermined difficulties in

techniques used in preparation of the samples. A high anisotropy similar to $GdCo_5$ was also noted.

Structure of the Compound $GdMn_5$

The study of Gd-Mn was initiated in order to produce a magnetic alloy with the extremely high saturation value (B_S = 25,400 gauss) of gadolinium but with a higher Curie temperature (Gd = 20°C). Consideration of atomic structures suggested that an alloy of 38% Gd and 62% Mn would meet these requirements. Magnetic measurements on this material indicated unusual spin behavior. The alloy structure of this composition seemed distinctly different from any other system previously studied. A complete crystal structure determination was undertaken in an attempt to explain the unusual magnetic behavior.

X-ray precession photographs were taken of a single crystal of a $GdMn_5$ compound. From this data the compound was found to have a face centered cubic lattice with a parameter of 12.58Å. It was possible for this lattice to belong to one of the following space groups, Fm3m, F432, Fm3 or F23. Since γ Mn belongs to space group Fm3m, a structure analysis was started assuming that our crystal also belonged to this same space group. From chemical analysis (63.5% Mn, 36.5% Gd) and density measurements (~ 8.8) made on powdered materials that were identified as having the same lattice parameters and coming from the same melt, it was possible to calculate the total number of atoms in the unit cell to be 120 Mn atoms and 24 Gd atoms. This is equivalent to 24 units of $GdMn_5$ in the cell.

The structure determination has so far placed the atoms as follows:

48 (i)	Mn	at coordinates	0.5	0.2	0.2
32 (f)	Mn	at coordinates	0.17778	0.17778	0.17778
32 (f)	Mn	at coordinates	0.37778	0.37778	0.37778
4 (b)	Mn	at coordinates	0.5	0.5	0.5
4 (a)	Mn	at coordinates	0	0	0
24 (e)	Gd	at coordinates	0.2	0	0

These values are not exact since they are based on powder data.

The best magnetic moment data we have obtained on 6 single crystals indicate a sigma for the material at 75°K of 124 which calculates out to be 232 bohr magnetons per unit cell at 75°K or a saturation magnetization of about 13,000 gauss. The Curie temperature was found to be about 200°C.

MAGNETIC MATERIALS

Measurements of Narrow Line Widths

A simple rapid method has been developed to measure very narrow line widths (0.5 oersteds). It is a modification of the method previously developed by Masters et al. A sample 10 mils or larger is inserted thru a hole in the side of a shorted waveguide at a position of zero electric field. At magnetic resonance the audio modulation from the reradiated microwave field produced by the sample resonance is detected from a loop and read on an audio voltmeter. For the narrow line width samples considered, a 3db attenuation in the waveguide produces the same voltmeter reading as would be produced by changing the resonant magnetic field to the half-power point on the resonant curve. Twice this difference in magnetic field is the line width. A comparison of this method with cavity perturbation techniques reveals consistently similar results. The major difficulty with the latter method is that the magnetic field must be held constant to 0.1 gauss in a field of 1500 gauss. By sweeping the magnetic field this difficulty is removed and photographic techniques can be employed. One double exposure photograph is taken with and without the 3db attenuation.

Materials Processing

An automatic sphere grinding and polishing technique has been developed for use with yttrium-iron garnet and similar materials. This apparatus is shown in Figure 9. This represents a solution to one of the problems encountered in the construction of ferromagnetic microwave amplifiers, oscillators, limiters and related devices. The entire grinding and polishing operation requires less than a day. The only manual operation required is the changing of abrasive sizes.

A highly polished sphere is produced with a spheroidicity of better than ± 0.0001 inches. Surface imperfections are nearly indistinguishable optically. The resonance line width of single crystal yttrium-iron garnet can be used as an indication of perfection in polishing. Line widths in the order of 0.5 oersteds are readily obtainable.

Magnetic Annealing of Al-Fe

As in the case with the iron-silicon soft magnetic alloy system, the aluminum-iron alloys were found to be quite responsive to magnetic annealing cycles, particularly in the composition range of 5% to 12% aluminum (by weight). For example, as indicated in Figure 10 an increase in maximum permeability value from 3,500 to 51,000 resulted by annealing an 8% aluminum-iron alloy in a magnetic field. These results were obtained from laminated ring cores made from fairly isotropic material having a thickness of 0.014 inches.

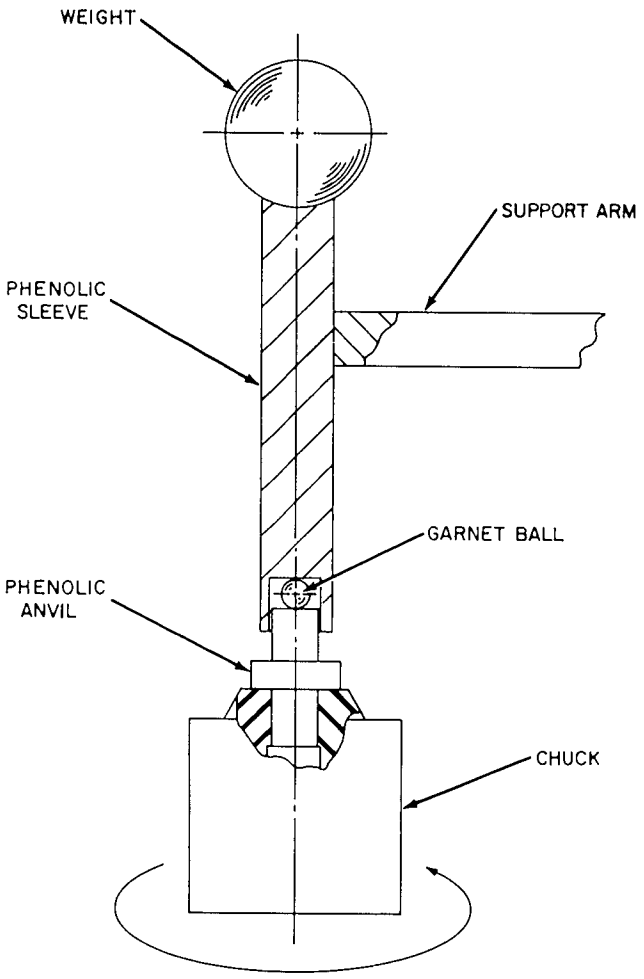

Fig. 9 Sphere Grinder

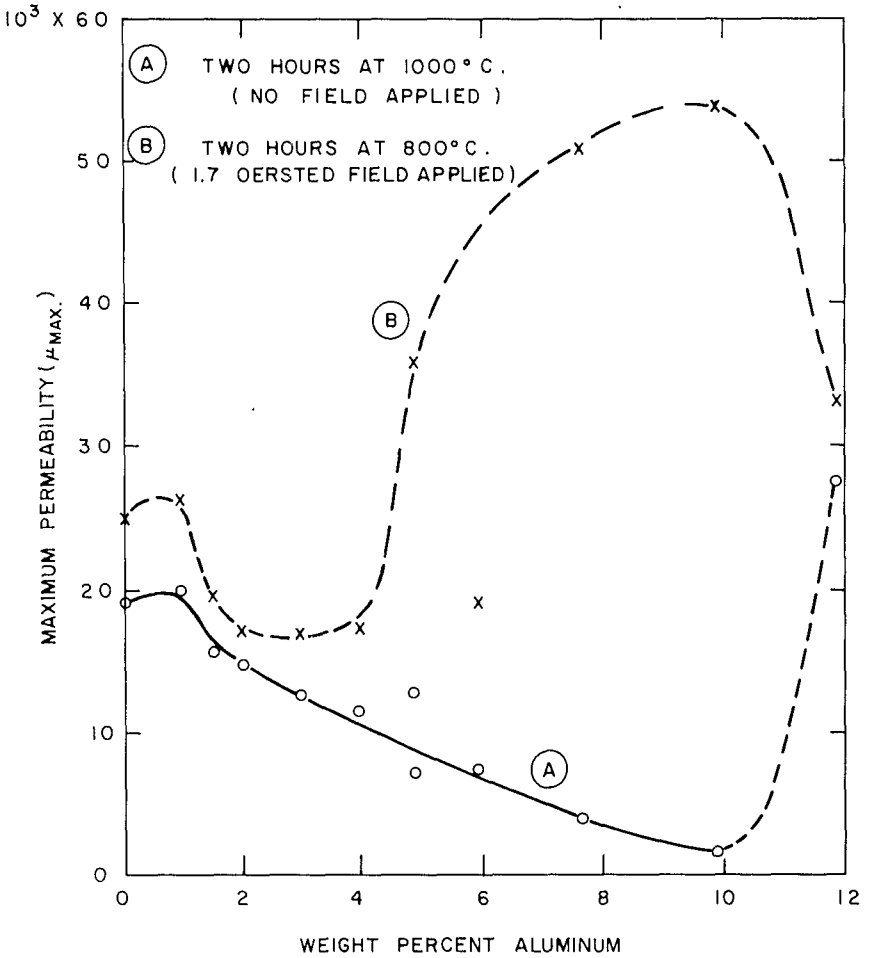

Fig. 10 Effect of magnetic anneal vs normal anneal on D-C permeability of iron-aluminum alloys (0.014 material).

High Pressure Research for Magnetic Materials

Since new materials and new forms of existing materials have been produced by the application of very high pressures and temperatures, it was decided to investigate the potential of these techniques for magnetic materials research.

After preliminary experiments were performed on cerium-iron compounds, using facilities at the National Bureau of Standards (NBS), a new cubic, multi-anvil apparatus, based on NBS design, was built and put into operation recently at NOL. Pressures in excess of 50 kilobars (kb) were obtained during calibration runs. This present upper limit is set by the hydraulic press capacity, rather than by the high pressure apparatus. Provision for simultaneous application of heat ($\sim$ 2,500°C) to the sample under pressure is a feature of this equipment.

Substituted Ferrites

Ferrimagnetism is characterized by materials with two or more magnetic and crystallographic sublattices usually designated A and B. The number and kind of atoms on the different sublattices determines the magnetic properties of the material. Measurements by X-ray diffraction and of the magnetic moments give an indication of the crystal line structure and the possible distribution of atoms on the sublattices.

We have studied the effect of substituting divalent zinc, which has no inherent magnetic moment, in a lithium manganese ferrite as:

$$\underset{1-2x-y}{Mn^{2+}}\ \underset{x}{Mn^{3+}}\ \underset{x}{Li^{+}}\ \underset{y}{Zn^{2+}}\ Fe_2O_4$$

It was expected that the substitution of zinc for the divalent manganese would reduce the moment of the A site and thus increase the net moment of the material, because the net moment is dependent on the difference between the moments of the A and B sites. As higher concentrations of lithium and zinc were substituted in the structure, a second phase, lithium ferrate resulted. This undesired second phase has now been eliminated, in some cases by a variation in the processing technique.

Preliminary data on the magnetic properties show that for the series $x = 0.1$; $y = 0$, .2, .4, and .6, the moment increases for values up to $y = 0.4$ and then falls off. The Curie temperature was found to decrease as expected. A single-phase spinel was formed in each case resulting in a decrease in the unit cell parameter with an increase of zinc substitution. These data indicate that the zinc is moving into the A sites and thus causing the expected results.

ENVIRONMENTAL MAGNETIC STUDIES

Nuclear Radiation Effects on Magnetic Materials

A comprehensive program to determine the effects of neutron radiation on "permanent" and "soft" magnetic materials was completed. This work is the first and only complete source of information on this subject. It has enabled the military establishments and their contractors to predict the performance of all types of magnetic devices for use in environments created by nuclear weapons and nuclear propulsion. Evidence of the utilization of the data generated by this work is shown by the continuing requests received by NOL for information concerning the application of magnetic materials in radiation environments.

A program has been started to determine the effects of charged particle radiation on magnetic materials.

High Temperature Nuclear Environment Resistant Magnetic Alloys

An investigation of the iron-aluminum alloy system containing low percentages of aluminum (0% to 10%) was conducted for the purpose of determining their usefulness in magnetic components exposed to unusual environments such as elevated temperatures, radiation from nuclear power sources, and extreme conditions of vibration, shock, pressure, and humidity. Results of magnetic data to date indicate this system of alloys to be slightly inferior to the iron-silicon soft magnetic alloy system; however, these two alloy groups must be rated exceptionally high when compared with other soft magnetic alloys as to resistance to the above environmental conditions.

One important advantage that the low percentage aluminum-iron alloy system offers over the silicon-iron system, and over most other soft magnetic alloy systems, is its room temperature ductility. A cold reduction of thickness of better than 98% can be obtained on aluminum-iron alloys containing up to 6% aluminum, by weight; this factor alone should make possible the economical production of thin gauge and/or crystal oriented materials.

The oxidation resistance of these soft magnetic iron alloys containing additions of aluminum, silicon, or combinations thereof also make these systems particularly promising for use in elevated temperature (500°C) open-air environments. Results obtained on four of these alloys, each containing approximately 4% alloy addition, are shown in Figure 11. As may be observed, the initial surface condition is a governing factor regarding rate of oxidation. The dry hydrogen pre-anneal produces surfaces on all alloys that afford best oxidation resistance during short-time exposures; however, for many applications it may be more desirable to use alloys that have previously been subjected to a preferential oxidation annealing cycle in wet hydrogen. This latter treatment provides a surface oxide that becomes relatively stable at some period within a 24-hour exposure cycle. All alloys containing aluminum and silicon demonstrated this same stability

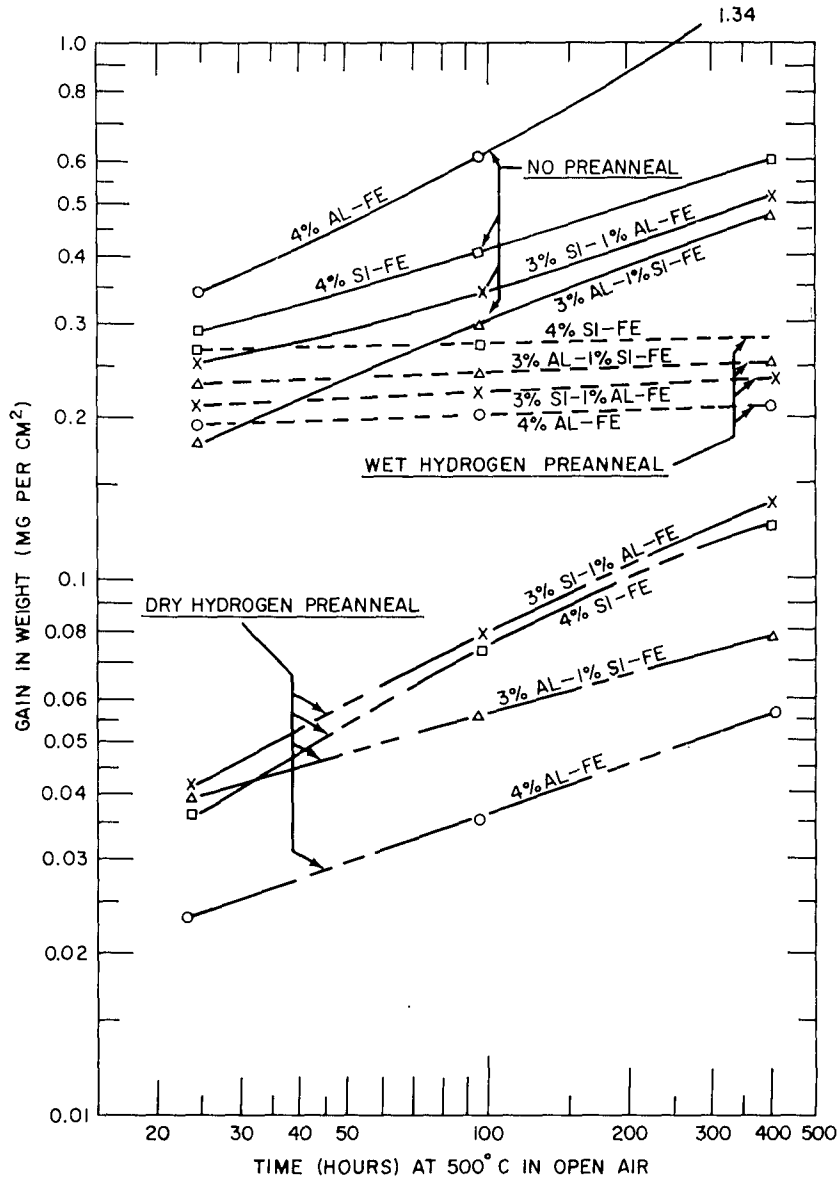

Fig. 11 Effects of preanneal on oxidation resistance of aluminum-iron, silicon-iron, and aluminum-silicon-iron magnetic alloys (0.014" material).

following the wet hydrogen anneal. The oxide formed during this preferential anneal was quite uniform and tenacious, therefore this technique may also be applied to materials used in other than magnetic applications.

THERMAL AND ELASTIC INVESTIGATIONS

Calculation of the Low Temperature Excess Specific Heat of SiO_2 Glass

The elastic constants do not account for all of the low temperature specific heat of SiO_2 glass although there is good agreement between elastic and thermal measurements of crystalline quartz. This suggests that a mechanism which is characteristic of the glassy state may be responsible for the low temperature excess specific heat. Because the large low temperature ultrasonic attenuation in silica glass is also absent in crystalline quartz, the possibility that both phenomena are due to the same structural unit was considered.

In an earlier study, a specific structural defect and an elongated Si-O-Si bond with two equilibrium positions for the bridging oxygen atom, was suggested as the ultrasonic relaxation loss mechanism. The potential energy of this extended bond can be approximated by the sum of two Morse potentials. This potential was used in a one-dimensional Schrodinger equation in solving for the vibrational energy levels of the extended bond. A set of split energy levels was found where the lowest pair results in a low temperature two state specific heat contribution which is in the proper temperature range to account for the anomaly. More than 25% of the total number of Si-O-Si bonds must be in this extended high energy state if this defect is responsible for all of the excess specific heat.

Effect of Fast Neutron Irradiation on the Temperature and Pressure Dependence of the Elastic Moduli of SiO_2 Glass

The temperature and pressure dependence of the elastic moduli of SiO_2 glass is anomalous. A comparative study was made of the effect of heavy fast neutron irradiation on this anomalous behavior and on the low temperature ultrasonic attenuation in order to investigate the possibility that both phenomena are associated with the same structural feature. The temperature and pressure dependence of the moduli was determined by measuring the change of the longitudinal and shear velocities using an ultrasonic phase interference technique at a frequency of about 50 mc/sec. The attenuation was determined by measuring the decrease of signal strength per round trip through the SiO_2 glass sample.

A sample of Amersil optical grade fused silica was irradiated to an integrated flux density in excess of 5×10^{19} n/cm^2. The ultrasonic loss peak was decreased to about 17% of its original value indicating the same percentage decrease in the structural units which contribute to this loss. Corresponding to this decrease, the anomalous temperature dependence of the compressibility changed from + 6.6% before irradiation to + 1.9% after

irradiation over a temperature range of from 100°K to 300°K while the pressure dependence of the compressibility at room temperature changed from + 5.4% before irradiation to + 2.1% after irradiation over a pressure range from atmospheric pressure to 5×10^4 psi. See Figure 12. Similar effects were found in the temperature and pressure dependence of the shear modulus. These results suggest that the same structural unit which is responsible for the low temperature ultrasonic relaxation loss may also be responsible for the anomalous behavior of the moduli.

Thermal Coefficients of Expansion of PbS, PbSe, PbTe, and SnTe

In addition to a number of direct applications in experimental work, the thermal coefficients of expansion of solids are useful in the analysis of certain types of data. For example, in experiments where mechanical work is done on the samples, these coefficients give the information required to convert the results from isothermal to adiabatic or vice versa, by thermodynamics. They also provide some of the information required for separating thermal effects into those due to lattice dilation and to a change in the distribution of excited states in the crystal.

Since these crystals are all cubic, they each have only one independent coefficient of thermal expansion. The coefficients of PbS, PbSe, PbTe and SnTe were determined from precision X-ray lattice parameters measured at 80 and 273°K. The lattice parameters were measured on annealed powder samples using the Debye-Scherrer photographic technique. The data below shows the resulting thermal coefficients which are all the same within experimental error.

Material	$\frac{1}{a}\frac{\Delta a}{\Delta t} \times 10^6$ °C
PbS	1.68 + 0.05
PbSe	1.70 + 0.06
PbTe	1.71 + 0.05
SnTe	1.76 + 0.10

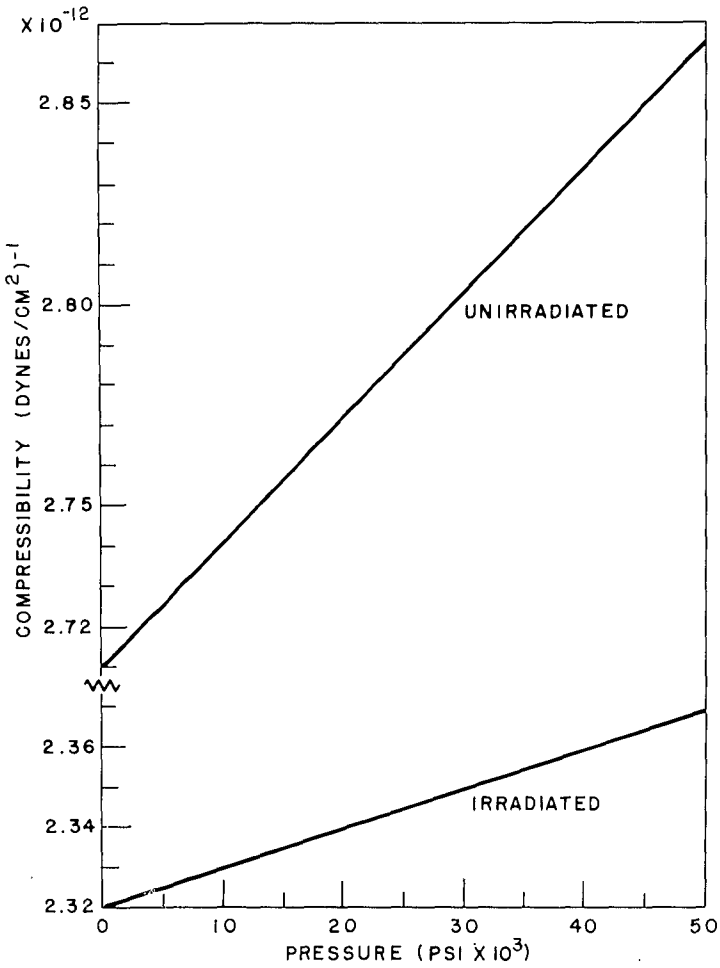

Fig. 12 Effect of heavy fast neutron irradiation on the anomalous pressure dependence of the compressibility of SiO_2 glass.

Elastic Constants of Single-Crystal YIG

Recent experiments on magnetostriction and magnetoacoustic interactions have shown the need for an accurate determination of the mechanical properties of single-crystal yttrium iron garnet (YIG). Although Young's modulus and velocity measurements have been made on polycrystalline YIG, anisotropic velocities or elastic constants cannot be calculated using these values.

A phase interference method was used to measure the shear and longitudinal ultrasonic velocity in a single crystal of YIG. The sample and a 7 Mc quartz crystal were bonded onto opposite ends of a fused silica delay line. The velocity was determined by measuring the frequencies at which constructive interference occurred between the signal reflected from the delay line-sample boundary and the signal that made return trips through the sample. Table V shows the elastic stiffness and compliance values calculated from these velocity measurements. A comparison between these values and the ones found for magnetite and Ni ferrite showed that the elastic anisotropy of YIG is much less than in the other two. Because this anisotropy is very small, the elastic properties of polycrystalline YIG could be calculated rather accurately from the single crystal elastic constants. The Lame constants, λ and μ, and the bulk modulus, determined in this manner were found to agree very well with the experimentally measured values. The linear magnetostriction due to magnetic dipole-dipole interaction, calculated from polycrystalline YIG using the single crystal elastic constants, was found to be -1.7×10^{-8}. This is an order of magnitude lower than the experimentally measured values.

TABLE V

ELASTIC MODULI AND STIFFNESS OF YIG

	c_{11}	c_{44}	c_{12}	s_{11}	s_{44}	s_{12}	
	(10^{-11} d/cm^2)			(10^{12} cm^2/d			$2c44/(c_{11}-c_{12}$
YIG	26.9	7.64	10.77	0.483	1.31	-0.138	0.947
Magnetite[a]	27.3	9.7	10.6	0.47	1.03	-0.131	1.16
Ni Ferrite[b]	22.0	8.12	10.94	0.68	1.23	-0.226	1.47

a. M. Doraiswami, Proc. Indian Acad. Sci. A25, 413 (1947)
b. D. Gibbons, J. Appl. Phys. 28, 810 (1957)

Acoustic Impedance Measurements in Indium at 1 and 10 Kmc

Our low temperature specific heat measurements of indium and niobium in the superconducting state have revealed a deviation from the $\alpha T^3 + \gamma T$ law. This can be explained by assuming that the energy of high frequency lattice vibrations increases as the metal becomes superconducting. If this is so, the increase should be reflected in a difference in wave number and velocity between phonons in the normal state and those of equal energy in the superconducting state if their wavelength is shorter than the coherence length (about 6,000 Å in indium). Therefore, velocity measurements of "sound" waves at microwave frequencies provide a test for this hypothesis and perhaps make it possible to predict which other superconductors, if any, exhibit this rare specific heat behavior.

The extension of high frequency ultrasonics into the kilomegacycle region is possible by surface exciting quartz rods in high electric fields (see Figure 13). There are two types of experiments from which the sound velocity can be determined: A reflection experiment in which the sound wave is bounced off of the material to be investigated and the velocity calculated from the reflection coefficient; and a transmission experiment in which the sound wave penetrates the material and the velocity is measured directly or by an interference technique. One and ten kmc velocity measur - ments in indium using the first method with both longitudinal and shear waves indicate the absence of any dispersion greater than 3%. This value is too small to account for all of the specific heat anomaly. As a result, transmission experiments are being planned to determine whether the lack of dispersion is characteristic of the entire sample or whether it is only found at the surface.

INTERMETALLIC COMPOUND INVESTIGATIONS

Intermetallic compounds offer possibilities for missile applications because of their low to moderate densities, high melting temperatures, excellent elevated temperature strength, high hardness, and good abrasion resistance. Brittleness, particularly at room temperature, of the higher melting temperature compound alloys continues as a major obstacle to the useful application of these materials. Consequently much of the investigative work on compound alloys was directed toward understanding and devising means of eliminating or circumventing the brittleness problem.

The principal studies were made on:

1. Homogeneous Compound Alloys (single-phase stoichiometric compounds)

2. Heterogeneous Compound Alloys (multi-phase alloys based upon an intermetallic compound)

In both of the above study areas powder metallurgy was employed to consolidate the materials. Hot pressing pre-alloyed compound powder was used to produce the high density single-phase compound alloys for further

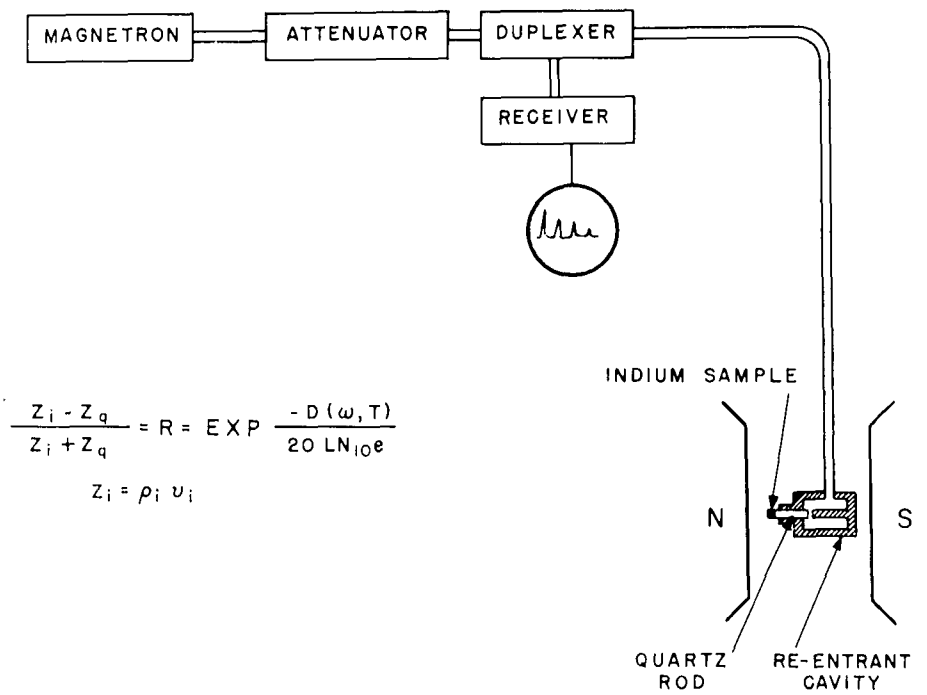

$$\frac{Z_i - Z_q}{Z_i + Z_q} = R = EXP \frac{-D(\omega, T)}{20 LN_{10} e}$$

$$Z_i = \rho_i v_i$$

Fig. 13 Block diagram of system to measure "sound" velocities at 10 kmc. Z_1 and Z_q represent the impedances of indium and quartz respectively and D (ω, T) represents the difference in db between two adjacent reflected pulses.

study, while the heterogeneous compound alloys will be produced by liquid-phase sintering techniques. The liquid media, for the liquid-phase sintering, will be either a pure metal, alloy, or another intermetallic compound. Preceeding the liquid-phase sintering work, fundamental studies on surface tension and wetting involving the intermetallic compounds was of interest. The sessile-drop method was employed in these studies. Based upon this sessile-drop investigation compatible heterogeneous alloy systems will be liquid-phase sintered and the resultant materials thoroughly studied.

MILITARY APPLICATIONS

Non-Magnetic Hand Tools for Ordnance Disposal

The U. S. Navy has been concerned for some time in obtaining suitable non-magnetic hand tools for use with magnetic-sensitive underwater ordnance devices. Previously these tools have been produced from beryllium-copper and copper-nickel-manganese alloys, both being hardenable by solid solution precipitation mechanisms. Tools when made from these alloys, however, have certain inherent mechanical property limitations either in hardness or ductility that seriously affect their life expectancy and efficiency. An entirely new alloy system has been developed to meet this need. These new alloys are based upon binary alloys of nickel and titanium and are mainly composed of the intermetallic compound NiTi and associated compounds $NiTi_2$ and Ni_3Ti. All of these compounds have been determined to be non-magnetic. Working in the alloy range of about 54 to 62 w/o Ni remainder Ti, a wide spectrum of mechanical properties were available. An example was the 60 w/o Ni-Ti alloy, which when quenched from 900 to 1050°C yielded a hardness of 62 Rc, yet the same alloy furnace cooled gave a hardness near 35 Rc. Intermediate hardnesses between 35 and 62 Rc, and the associated increases in toughness, were made possible by employing pseudo-tempering treatments.

Currently, unavailable mechanical property data on the arc-cast and wrought alloys from 54 to 62 w/o Ni-Ti are being obtained. These data, plus existing data, will be employed in the materials selection, heat treatment, and mechanical design of many common non-magnetic hand tools. It is intended that the hand tools so produced will be exhaustively tested, both mechanically and magnetically, utilizing in many cases the appropriate rigid ASTM standard tests and procedures.

A New Type Flux-Gate Magnetometer

A new flux-gate sensing element has been developed. It is a type of second-harmonic flux-gate magnetometer utilizing a toroidal core in which the alternating current excites alternating flux over a gapless magnetic path. The external magnetic field was sensed with respect to its reference axis by the suitable placement of the detector windings. This device was normally operated from a square-wave producing transistor-magnetic multivibrator. The toroidal magnetometer element controlled the frequency of oscillation.

The advantages inherent in this sensor over the more conventional rods or strips of magnetic material were:

1. No adverse magnetic remanence effects due to the gapless path were presented to the alternating flux.

2. The power drain of the device was very low due to the gapless feature. It was of the order of 20 milliwatts.

3. The mechanical strength associated with the tape winding or laminated toroidal structure permitted a rather large effective length to diameter ratio of the effective sensing portions of the magnetic circuit.

By using Supermalloy cores having an inside diameter of 1 1/4" and an ID-OD ratio in the range of 0.90 to 0.98, a sensitivity of 1,000 microamps/oersted or 1 volt/oersted was achieved. In special cases, the inside diameter of ultra-thin, 1/8 mil tape cores was reduced to 0.5 in., or less, to permit "point measurements" on small volumes of inhomogeneous magnetic factors.

The ring core permitted operation at the higher excitation frequencies. These higher frequencies were supplied by a magnetic-coupled transistor multivibrator. The complete circuit of multivibrator and magnetometer is shown in Figure 14.

Two modifications of this magnetometer presently of interest are:

1. A single component magnetometer with cosine law directivity characterized by extreme simplicity and low power drain

2. An omnidirectional magnetometer (senses omnidirectionally the field components in a given plane) produced by multiple sets of detector windings on a single core with a simple summing circuit.

Low Signal Level Magnetic Amplifiers

Magnetic amplifiers have been developed and supplied for use in instrumentation applications. These devices have in addition been employed in certain missile applications. They are ultra-stable high gain devices operating from input powers in the order of 10^{-8} watts for full-scale deflection of output instrument.

Such a self-balancing low-level, push-pull type, magnetic amplifier having a voltage gain of 100, i.e., 0.02:2 volts ac, has been developed to be used in the HASP program. Other forms of this amplifier are designed for an output current of 0...±100 microamps (load resistance: 100 to 2,000 ohms) and for a corresponding d-c input signal of 0...1 millivolt or 0...1 microampere, respectively. The drift rate of these amplifiers is of the order of 10^{-13} watts for room temperature changes.

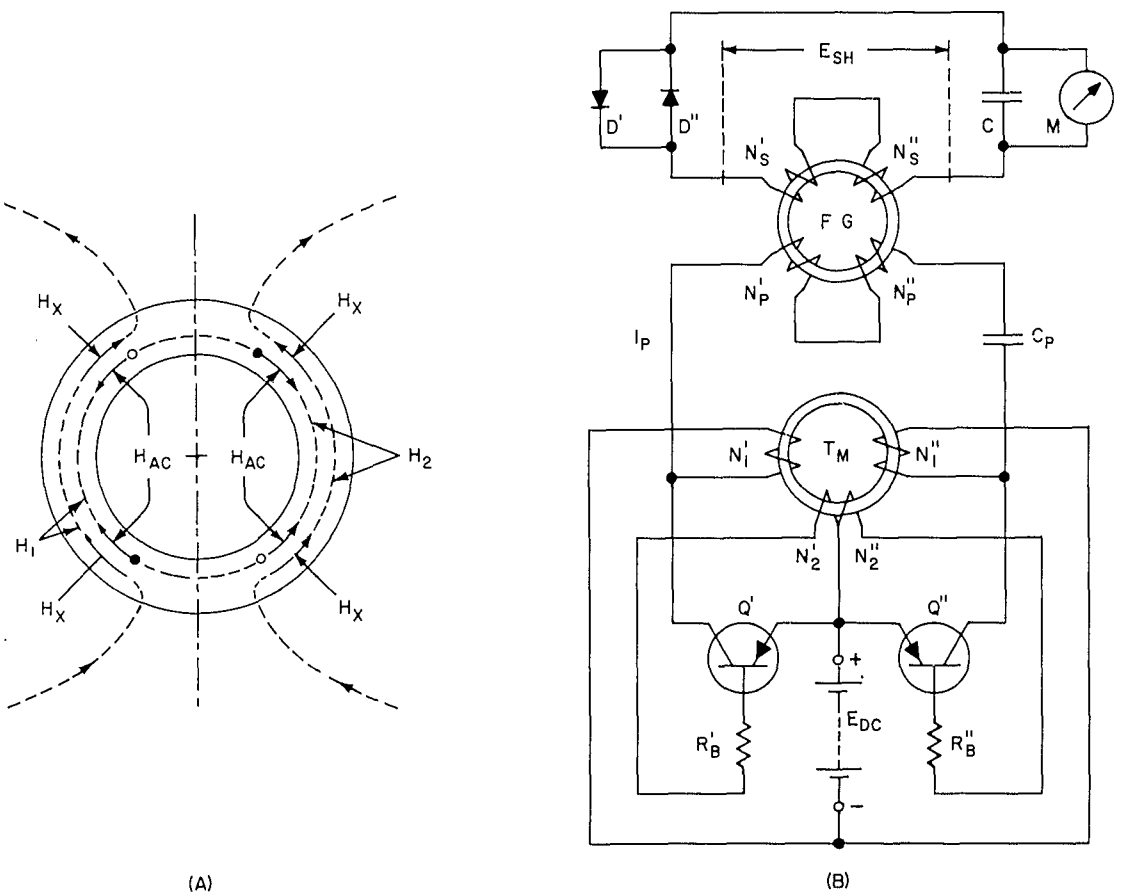

Fig. 14 Ring-core flux-gate magnetometer. (A) Fundamental principle. (B) ac excitation with switching-transistor magnetic-coupled multivibrator.

Design and Construction of Attitude Correcting Solenoids for the TRAAC Satellite

Electromagnetic solenoids were designed upon request of the Johns Hopkins Applied Physics Laboratory for use in the TRAAC Satellite. These solenoids develop torque on the earth's magnetic field to change the attitude of the satellite with respect to the earth. When the solenoid current is turned off the magnetic material is required to be demagnetized in order to produce minimum torque.

The solenoids were required to produce a moment of 4×10^4 to 9×10^4 pole-cm (cgs units) when perpendicular to the field and when excitation was removed to produce less than 100 pole-cm of moment. Available power was 3.5 watts and the upper weight limit was 10 pounds. A capacitor discharge system was designed to demagnetize the magnetic material when excitation was removed from the solenoid.

The advantages of this system over others under consideration were:

1. System was reusable after initial correction was complete

2. Magnetic material was designed for very moderate but stable performance making it insensitive to shock, vibration, and external fields

3. Demagnetizing circuit was simple and dependable requiring very little energy.

Units were constructed and supplied to the Applied Physics Laboratory for installation in the TRAAC Satellite which was orbited November 15. Figure 15 shows the solenoids installed in the satellite.

NON-LINEAR CIRCUITRY

A New Principle of Detection

A new principle of detection has been established. This relates to the use of a circuit element having a cube-law characteristic for the detection of modulation present in an asymmetric voltage. This type of voltage waveshape is fairly common and is produced by a class of non-linear circuits which include thyratrons, controlled rectifiers, and magnetic amplifiers of the type which operate on the flux-current (B-H) loop of a magnetic material. A symmetrical non-linear resistance has a cube-law characteristic and although it is useless as a detector for symmetric voltage waveshapes it is found to have the necessary characteristic for polarity sensitive detection of asymmetric voltage waveshapes.

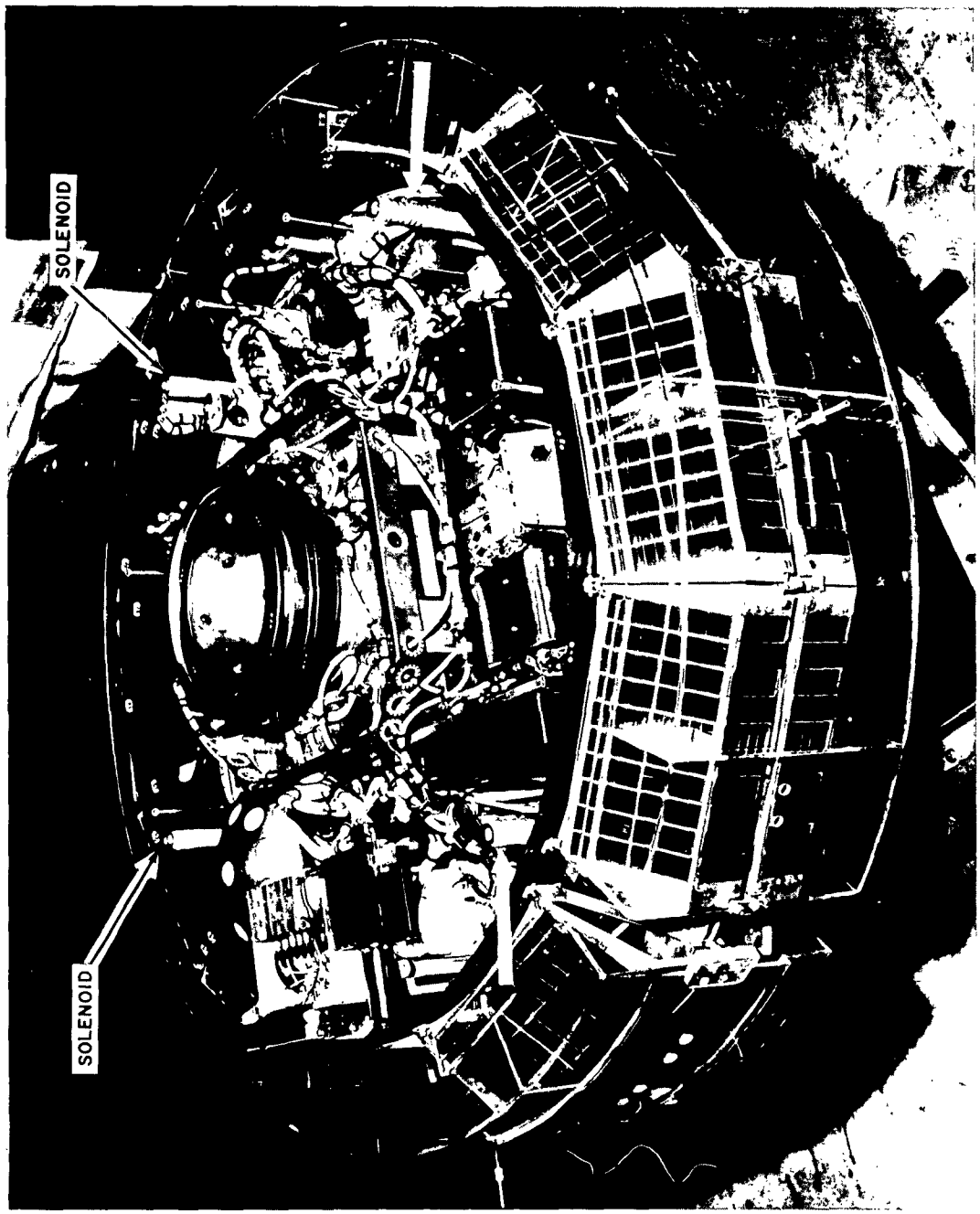

Fig. 15 TRAAC Satellite showing the electromagnetic solenoids.

Principles of Amplification

The mechanisms of pumping and coupling in oscillating systems have been set forth for use in the field of parametric amplification. These mechanisms are the underlying principles of operation of varied devices such as the semiconductor varactor microwave amplifier and the ferromagnetic yttrium-iron garnet microwave amplifier.

The stable gain properties predicted by the conservation theorems of Manley-Rowe for the upper sideband case of the three-frequency parametric amplifier and the regenerative effects associated with the lower sideband case have been explained in terms of feedback theory.

REPORTS AND PUBLICATIONS

Naval Ordnance Laboratory Reports

Alperin, H. A., and Pickart, S.J. - "Antiferromagnetic Compounds," NOLTR 61-18, 10 April 1961

Buehler, W. J., and Wiley, R. C. - "The Properties of TiNi and Associated Phases," NOLTR 61-75, 1 July 1961

Dayhoff, E. S., Treacy, E., and McGuire, T. R. - "Nickel Ferrite and Related Materials," NavOrd Report 6922, 1 July 1960

Gordon, D. I. (See Sery, R)

Hooper, E. T., and Lundsten, R. H. - "Design and Construction of Attitude Correcting Solenoids for the TRAAC Satellite," NOLTR 61-120

Lundsten, R. H. (See Sery, R. S.)

_____ (See Hooper, E. T.)

Maxwell, L. R. - "Solid State Research of the Applied Physics Department for the Year 1960," NOLTR 61-49, 29 May 1960

McGuire, T. R. - (See Dayhoff, E.S.)

Morrison, R.E. - "Reflectivity and Optical Constants of Indium Arsenide, Indium Antimonide and Gallium Arsenide," NOLTR 61-56, 1 July 1961

Pickart, S. J. - (See Alperin, H.A.)

Sery, R. S., Lundsten, R. H. and Gordon, D. I. - "Radiation Damage Thresholds for Permanent Magnets," NOLTR 61-45, 18 May 1961

Treacy, E. - (See Dayhoff, E. S.)

Wiley, R. C. - (See Buehler, W. J.)

Papers and Abstracts Published

Allgaier, R. S. - "Galvanomagnetic Effects and Band Structure in PbS, PbSe, and PbTe," Proceedings of the International Conference on Semiconductor Physics, Prague, 1960 (Publishing House of the Czechoslovak Academy of Sciences, Prague, 1961) p 366

_____, "Valence Bands in Lead Telluride," J. Appl. Phys. 32, 2185S (1961)

_____, (See Burke, J. R.)

_____, and Scheie, P. O. - "Electrical Properties of p-Type SnTe," Bull. Am. Phys. Soc. 6, 436 (1961)

Alperin, H. A. - "Aspherical 3d Electron Distribution in Ni^{++}," Phys. Rev. Letters 6, 55 (1961)

Bis, R. F. - "Temperature-Pressure Projection of the Three-Phase Line of Lead Telluride," M.S. Thesis, Univ. of Md., June 1961

_____, (See Houston, B. B.)

Brebrick, R. F. - "Composition Stability Limits of Binary Semiconductor Compounds," Phys. Chem. Solids 18, 116 (1961)

Burke, J. R., Jr., Houston, B. B., Jr., and Allgaier, R.S. - "Room-Temperature Piezoresistance and Elastoresistance in p-Type PbTe, " Bull. Am. Phys. Soc. 6, 136 (1961)

Callen, E. R. - "Anisotropic Curie Temperature," J. Appl. Phys. 32, 221S (1961)

_____, "Anisotropic Curie Temperature," Phys. Rev. 124, 1373 (1961)

Clark, A. E. and Strakna, R. E. - "Elastic Constants of Single Crystal YIG," J. Appl. Phys. 32, 1172 (1961)

Davis, J. L. - "Production of a Low Surface Recombination Velocity on <111> Faces of n-Type Indium Antimonide at 77°K," Bull. Am. Phys. Soc. 6, 18 (1961)

Dayhoff, E. S., - "Electromagnetic Modes of an Optical Maser," Bull. Am. Phys. Soc. 6, 365 (1961)

Dixon, J. R. - "Optical Absorption Mechanisms in Indium Arsenide," Proceedings of the International Conference on Semiconductor Physics, Prague, 1960 (Publishing House of the Czechoslovak Academy of Sciences, Prague, 1961) p 366

_____, and Ellis, J. M. - "Optical Properties of n-Type Indium Arsenide in the Fundamental Absorption Edge Region," Phys. Rev. 123, 1560 (1961)

_____, "Reflectivity of p-Type Lead Telluride in the Infrared Region," Bull. Am. Phys. Soc. 6, 312 (1961)

Edwards, P. L., and Happel, R. J., Jr. - "Sapphire Whisker Growth on a Single-Crystal Substrate," Bull. Am. Phys. Soc 6, 24 (1961)

_____, "Whisker Rotation Apparatus for Polarizing Microscope," Rev. Sci. Instr. 32, 95 (1961)

Ellis, J.M., Jr. - (See Dixon, J. R.)

Ferebee, S. F. - (See McGuire, T. R.)

Gordon, D. I. - "Environmental Evaluation of Magnetic Materials," Electro-Technology 67, No. 1, 118 (Jan. 1961)

Greene, R. F. - "Surface Dependence of the Thermoelectric Power in Germanium at Room Temperature: Theoretical," Bull. Am. Phys. Soc. 6, 27 (1961)

_____, (Y. Goldstein, N.B. Grover, A. Many, and R. F. Greene)- "Improved Representation of Calculated Surface Mobilities in Semiconductors. II. Majority Carriers," J. Appl. Phys. 32, 2538 (1961)

_____, (See Zemel, J. N.)

Gubner, E., (See Houston, B. B.)

Happel, R. J., (See Edwards, P. L.)

_____, (See Heikes, R. R.)

Heikes, R. R., McGuire, T. R., and Happel, R. J. - "The Role of Double Exchange in the Magnetic Structure of $Li_xMn_{1-x}Se$," Phys. Rev. 121, 703 (1961)

Houston, B. B., Jr. - "Stoichiometry of Melt-Grown Compound-Semiconductor Crystals," Fifth Navy Science Symposium, ONR-9, 2, 627 (1961)

_____, (See Burke, J. R.)

_____, Bis, R. F. and Gubner, E. - "Preparation of SnTe Single Crystals," Bull. Am. Phys. Soc. 6, 436 (1961)

Jensen, J. D. and Zemel, J. N. - "Electrical PbS Films: Electrical Properties," Bull. Am. Phys. Soc. 6, 437 (1961)

Litovitz, T. A., (See Slie, W. M.)

McGuire, T. R. and Ferebee, S. F. - "Magnetic Moments and Curie Temperatures of Lithium Substituted Manganese Ferrite," Bull. Am. Phys. Soc. 6, 53 (1961)

_____, (See Heikes, R. R.)

_____, (See Dayhoff, E. S.)

Morrison, R. E. - "Reflectivity and Optical Constants of Indium Arsenide, Indium Antimonide, and Gallium Arsenide," Phys. Rev. 124, 1314 (1961)

Norr, M. K. - "The Lead Salt Thiourea Reaction," J. Phys. Chem. 65, 1278 (1961)

Pickart, S. J. (R. Nathans, S. J. Pickart, and A. Miller) - "Field Dependence of the Magnetic Scattering in $CuCr_2O_4$," Bull. Am. Phys. Soc. 6, 54 (1961)

_____, Nathans, R., and Shirane, G. - "Magnetic Structure Transitions in $Li_xMn_{1-x}Se$," Phys. Rev. 121, 707 (1961)

_____, and Nathans, R. - "Unpaired Spin Density in Ordered Fe_3Al," Phys. Rev. 123, 1163 (1961)

Riedl, R. - "Infrared Absorption Beyond the Fundamental Absorption Edge in PbS and PbTe, " Bull. Am. Phys. Soc. 6, 312 (1961)

Scanlon, W. W. - "Properties of Heavy Atom Semiconductors," Semiconductor Nuclear Particle Detectors, NAS-NRC Publication 871, 145 (1961)

_____, "Solid State Research," Fifth Navy Science Symposium, ONR-9 2, 250(1961)

Scheie, P. O., (See Allgaier, R. S.)

Scott, E. J. and Zemel, J. N. - "Magneto-Surface Measurements on Germanium at Dry Ice Temperatures," Bull. Am. Phys. Soc. 6, 27 (1961)

Stern, F. - "Calculation of Optical Absorption in III-V Semiconductors," Proceedings of the International Conference on Semiconductor Physics, Prague, 1960 (Publishing House of the Czechoslovak Academy of Sciences, Prague, 1961) p 363

_____, "Aspherical 3d Electron Distribution in Body-Centered Cubic Metals," Phys. Rev. Letters 6, 675 (1961)

_____, "Optical Properties of Lead-Salt and III-V Semiconductors," J. Appl. Phys. 32, 2166S (1961)

Slie, W. M. and Litovitz, T. A. - "Effect of Alcohol Impurity on Ultrasonic Vibrational Relaxation in Liquid CS_2," J. Acous. Soc. Am. 10, 33 (1961)

Strakna, R. E. - "Investigation of Low Temperature Ultrasonic Absorption in Fast Neutron Irradiated SiO_2 Glass," Phys. Rev. 123, 2020 (1961)

_____, (See Clark, A. E.)

Strong, S. L. - "Crystal Structure Distortions in MnO_2 and MnF_2 at their Antiferromagnetic Curie Temperature," J. Phys. Chem. Solids 19, 51 (1961)

Wangness, R. K. - "Longitudinal Ferrimagnetic Resonance," Phys. Rev. 121, 472 (1961)

Zemel, J. N. - "Surface Dependence of the Thermoelectric Power in Germanium at Room Temperature: Experimental," Bull. Am. Phys. Soc. 6, 27 (1961)

_____, and Greene, R. F. - "Semiconductor Surface Transport," Proceedings of the International Conference on Semiconductor Physics, Prague, 1960 (Publishing House of the Czechoslovak Academy of Sciences, Prague, 1961)

_____, (See Jensen, J. D.)

PAPERS PRESENTED AT MEETINGS OUTSIDE THE LABORATORY

In the United States

Adams, E. - "Recent Developments in Soft Magnetic Alloys," 7th Annual Conference on Magnetism & Magnetic Materials, Phoenix, Arizona, 13-16 November 1961

_____, "Magnetic Properties of Materials," Navy Research and Dev. Clinic, Raton, New Mexico, 27-29 Sept. 1961

Allgaier, R. S. - (See Burke, J. R., Jr.)

_____, "Valence Bands in Lead Telluride," Conf. on Semiconducting Compounds, Schenectady, New York, 14-16 June 1961

_____, and Scheie, P. - "Electrical Properties of p-Type SnTe," Amer. Physical Society, Chicago, Ill., 24-25 November 1961

Alperin, H. A. - "The Form Factor of Nickel Oxide," Univ. of Connecticut Physics Colloquium, Storrs, Conn., 14 April 1961

Bis, R. F., Jr., (See Houston, B.B., Jr.)

Burke, J. R., Jr., Houston, B. B., Jr., and Allgaier, R. S. - "Room Temperature Piezoresistance and Elastoresistance in p-Type PbTe," American Physical Society, Monterey, California, 20-23 March 1961

Callen, E. R. - "Magnetoelastic Effect in Crystals," Department of Physics Colloquium, Univ. of Delaware, 4 March 1961; Dept. of Electrical Engineering, Univ. of Minnesota, 20 April 1961

_____, "Magnetoelastic Coupling in Cubic Crystals," Solid State Seminar, National Bureau of Standards, 8 Nov. 1961

Clark, A. E. and Strakna, R. E. - "Low Temperature Specific Heat in SiO_2 Glass Based on a Single Two State Model," Seminar at American Standard Co., Union, New Jersey, 17 October 1961

Davis, J. L. - "Production of a Low Surface Recombination Velocity on <111> Faces of n-Type Indium Antimonide at 77°K, "American Physical Society, New York, 1-4 February 1961

Dixon, J. R. - "Reflectivity of p-Type Lead Telluride in the Infrared Region," American Physical Meeting, Washington, D. C., 24-27 April 1961

Edwards, P. L. and Happel, R.J., Jr. - "Sapphire Whisker Growth on a Single-Crystal Substrate," American Physical Society Meeting, New York, 1-4 February 1961

Ferebee, S. F., (See McGuire, T. R.)

Geyger, W. A. - "Low-Level Magnetic Amplifiers," 17th Annual National Electronics Conference, Chicago, Ill., 9-11 October 1961

_____, "New Type of Flux-Gate Magnetometer," 7th Annual Conf. on Magnetism & Magnetic Materials, Phoenix, Arizona, 13-16 Nov. 1961

_____, "Comparison of Directly and Indirectly Measured Control Characteristics of Mag. Amplifiers with External Feedback," AIEE Summer General Meeting, Ithaca, New York, 18-27 June 1961

Greene, R. F. - "Surface Dependence of the Thermoelectric Power in Germanium at Room Temperature: Theoretical," American Physical Society Meeting, New York, 1-4 February 1961

Gubner, E., (See Houston, B.B., Jr.)

Happel, R.J., Jr., (See Edwards, P.L.)

Houston, B.B., Jr., (See Burke, J.R., Jr.)

_____, "Stoichiometry of Melt-Grown Compound-Semiconductor Crystals," Fifth Navy Science Symposium, Annapolis, Maryland, 18-20 April 1961

_____, Bis, R.F. and Gubner, E., - "Preparation of SnTe Single Crystals," American Physical Society Meeting, Chicago, Illinois, 24-25 November 1961

Jensen, J.D. and Zemel, J.N. - "Epitaxial PbS Films: Electrical Properties," American Physical Society Meeting, Chicago, Illinois, 24-25 November 1961

McGuire, T. R. and Ferebee, S.F. - "Magnetic Moments and Curie Temperatures of Lithium Substituted Manganese Ferrite," American Physical Society Meeting, 1-4 February 1961

McKee, H.W. - "NOL Solid State Devices Program," Navy Laboratory Microelectronics Program Conference, Silver Spring, Maryland, 12-13 June 1961

Pickart, S. J. (R. Nathans, S. J. Pickart, and A. Miller) - "Field Dependence of the Magnetic Scattering in $CuCr_2O_4$," American Physical Society Meeting, New York, 1-4 February 1961

_____, and Nathans, R. - "Magnetic Electron Density Maps by Neutron Diffraction," American Crystallographic Association Meeting, Boulder, Colorado, 31 July - 4 August 1961

_____, and Nathans, R. - "Alloys of the First Transition Series with Palladium and Platinum," Conference on Magnetism & Magnetic Materials, Phoenix, Arizona, 13-16 November 1961

Riedl, H. R. - "Infrared Absorption Beyond the Fundamental Absorption Edge in PbS and PbTe," American Physical Society Meeting, Washington, D. C., 24-27 April 1961

Scanlon, W. W.- "Solid State Research," Fifth Navy Science Symposium, Annapolis, Maryland, 18-20 April 1961

Scott, E. J. and Zemel, J. N. - "Magneto-Surface Measurements on Germanium at Dry Ice Temperatures," American Physical Society Meeting, New York, 1-4 February 1961

Stern, F. - "Energy Bands and Charge Distribution in Transition Metals," American Physical Society Meeting, Wash., D. C., 24-27 April 1961 (invited paper)

_____, "Optical Properties of the Lead Salts and the III-V Semiconductors," Conference on Semiconducting Compounds, Schenectady, New York, 14-16 June 1961

_____, "Neutron Diffraction Form Factors in Transition Metals," Univ. of Maryland Theoretical Physics Colloquium, 4 Oct. 1961

Strakna, R. E., (See Clark, A. E.)

Varela, J. O. (See Zemel, J.N.)

Zemel, J. N. - "Surface Dependence of the Thermoelectric Power in Germanium at Room Temperature: Experimental," Amer. Physical Society Meeting, New York, 1 February 1961

_____, (See Scott, E.J.)

_____, and Varela, J.O. - "Field Effect Studies on PbS Films," International Conf. on Photoconductivity, Bell Telephone Laboratories, Murray Hill, N.J., 21-24 August 1961

_____, "Semiconductor Surfaces," New York State Section of American Physical Society Meeting, Niagara Falls, 12-14 October 1961 (invited paper)

_____, (See Jensen, J.D.)

In Foreign Countries

Adams, E. - (See Hubbard, W.M.)

Alperin, H.A. - "Magnetic Form Factor of Nickel Oxide," International Conference on Magnetism and Crystallography, Kyoto, Japan, 25-30 Sept. 1961

_____, (See Pickart, S.J.)

Dayhoff, E. W. - "Electromagnetic Modes of an Optical Maser," American and Mexican Physical Society Meeting, Mexico City, Mexico, 22-24 June 1961

_____, "High Speed Photographs of a Ruby Laser," American and Mexican Physical Society Meeting, Mexico City, Mexico, 22-24 June 1961 (Post-deadline paper)

Hubbard, W. M. and Adams, E. - "Intermetallic Compounds of Iron and Cobalt with Gadolinium," International Conf. on Magnetism & Crystallography, Kyoto, Japan, 25-30 Sept. 1961

Pickart, S. J. (R. Nathans, S. J. Pickart and H. A. Alperin) - "Spin Density Distributions and Hartree-Fock Calculations for the Iron Group Series," International Conference on Magnetism & Crystallography, Kyoto, Japan, 25-30 September 1961

DISTRIBUTION

	Copies
Chief, Bureau of Naval Weapons Navy Department, Washington 25, D. C. Attn: Technical Library (DLI-3) R-12 R-13 RAAV-11 RM-12 RMGA-8 RMWC-432 RMWC-51 RREN-3 RREN-13 RREN-4 RRMA-2 RRMA-3 RU	2
Chief, Bureau of Ships Navy Department, Washington 25, D. C. Attn: Code 687C3 Code 681A2A Code 687C Code 681A1A	
Office of Naval Research Navy Department, Washington 25, D. C. Attn: Material Sciences Division (Code 419)	
Commanding Officer Office of Naval Research Branch Office 495 Summer Street Boston 10, Massachusetts Attn: T. B. Dowd	
Commanding Officer Office of Naval Research Branch Office 86 E. Randolph Street Chicago 1, Illinois Attn: Lloyd A. White	
Commanding Officer Office of Naval Research, Pasadena Branch 1030 East Green Street Pasadena 1, California Attn: Technical Library	

Director, U. S. Naval Research Laboratory
Washington 25, D. C.
Attn: Library (Code 2027)
Code 7350
Code 6450
Code 6470 (R. Wallis)

Commanding Officer
U. S. Naval Avionics Facility
Indianapolis, Indiana
Attn: Library

Commander, U. S. Naval Ordnance Test Station
China Lake, California
Attn: Technical Library
B. O. Serophin

Commanding Officer, U. S. Naval Ordnance Laboratory
Corona, California
Attn: Library
R. F. Potter

Commanding Officer and Director
U. S. Navy Electronics Laboratory
San Diego 52, California
Attn: Library

Office of Director of Defense Research and Engineering
Washington 25, D. C.
Attn: Materials Division

Directorate of Solid State Sciences
Air Force Office of Scientific Research
Washington 25, D. C.

Headquarters, U. S. Air Force
Washington 25, D. C.
Attn: AFDRD-RD

Hq. Detachment 2, Air Force Research Division (ARDC)
U. S. Air Force, Laurence G. Hanscom Field
Bedford, Massachusetts
Attn: Document Unit (CRRPL-3)

Commanding General, Frankford Arsenal
Philadelphia 37, Pennsylvania
Attn: Library, Reports Section, #0270

Office of the Chief Signal Officer
Research and Development Division
Washington 25, D. C.
Attn: Signal Research Office

Commanding Officer, Diamond Ordnance Fuze Laboratories
Washington 25, D. C.
Attn: Technical Reference Br. (ORDTL 012)

National Aeronautics and Space Administration
1520 H Street, N. W.
Washington 25, D. C.
Attn: Library/BIL 7

National Aeronautics and Space Administration
Lewis Research Center
21000 Brookpark Road
Cleveland 35, Ohio
Attn: Library

Director, National Security Agency
Fort George G. Meade, Maryland
Attn: Captain A. M. Cole (REMP-2)
Miss Savakinas (CREF-332) Rm. 2C087

National Bureau of Standards
Washington 25, D. C.
Attn: Library
H. P. Frederikse

ASTIA (TIPCR)
Arlington Hall Station
Arlington 12, Virginia 10

Westinghouse Research Laboratories
Pittsburgh 35, Pa.
Attn: J. M. Fertig, Head, Tech. Inf. 2
M. Garbuny, Optical Physics Section

Westinghouse Electric Corp.
Research Dept.
Bloomfield, N.J.
Attn: H. F. Ivey
P. Jaffe

Xerox Corp.
Research Laboratories
Webster, New York
Attn: E. M. Pell

Argonne National Laboratory
9700 South Cass Ave.
Argonne,Illinois
Attn: Hoylande D. Young

Armour Research Foundation
Chicago 16, Illinois
Attn: James J. Brophy (Asst. Mgr., Physics Research)

University of Arizona
Dept. of Physics
Tucson, Arizona
Attn: Roald K. Wangsness

Dept. of Physics
Carnegie Institute of Technology
Pittsburgh 13, Pa.
Attn: Library

Documents Department
General Library
Univ. of Calif.
Berkeley 4, Calif.

Univ. of Calif.
La Jolla, San Diego, Calif.
Attn: W. Kohn, Dept. of Physics

Cornell Univ.
Ithaca, New York
Attn: L. G. Parratt, Chairman, Dept. of Physics
Library

George Washington University
Washington, D. C.
Attn: T. P. Perros, Chemistry Dept.

Gordon McKay Library, Harvard Univ.
Div. of Eng. & Applied Physics
Pierce Hall, Oxford St.
Cambridge 38, Mass.
Attn: Tech. Reports Collection

Univ. of Illinois
Urbana, Illinois
Attn: R. J. Maurer, Dept.of Physics
Documents Division-ML, Univ. Library

Applied Physics Lab., Johns Hopkins Univ.
8621 Georgia Ave.
Silver Spring, Md.
Attn: G. L. Seielstad, Super. Tech. Rpts. Grp.
C. K. Jen

Radiation Laboratory, Johns Hopkins Univ.
1315 St. Paul St.
Baltimore, Maryland

University of Maryland
Dept. of Physics
College Park, Maryland
Attn: Richard Ferrell

Lincoln Laboratory
Mass. Institute of Technology
Box 73, Lexington 73, Mass.
Attn: Library, A-229
B. Lax

Mass. Institute of Technology
Cambridge 39, Mass.
Attn: Wayne B. Nottingham, Rm. 6-205
Laboratory for Insulation Research, Rm. 4-244
Research Lab. of Electronics, Rm. 26-327

Michigan State University
Physics Dept.
East Lansing, Michigan
Attn: C. D. House
R. D. Spence

University of Rochester
Rochester 20, New York
Attn: D. L. Dexter, Institute of Optics
D. Dutton
K. Teegarden

Texas Christian University
Physics Dept.
Fort Worth, Texas
Attn: P. L. Edwards

American Optical Co., J. W. Fecker Div.
6592 Hamilton Ave.
Pittsburgh 6, Pa.
Attn: W. Lewis Hyde

American Optical Company, Research Center
Southbridge, Mass.
Attn: Library

Avco Mfg. Corp. Research Laboratories
2385 Revere Beach Parkway
Everett 49, Mass.

Baird-Atomic, Inc.
33 University Rd.
Cambridge 38, Mass.
Attn: Library

Battelle Memorial Institute
Columbus 1, Ohio
Attn: A. C. Beer, Solid State Physics

Bausch & Lomb Optical Co.
635 St. Paul St.
Rochester, New York
Attn: Dr. Foster

Bell Telephone Laboratories
Murray Hill, N.J.
Attn: J. A. Morton

Bell Telephone Laboratories
Serial Assistant
Technical Information Libraries
463 West St.
New York 14, N.Y.

Clevite Research Center
540 East 105th St.
Cleveland 8, Ohio
Attn: Hans Jaffe, Electronic Research Div.

E. I. duPont de Nemours & Co.
Photo Products Dept.
Parlin, N.J.

Attn: Library

Minnesota Mining & Mfg. Co.
2031 Hudson Road
St. Paul 6, Minnesota
Attn: Library
F. A. Hamm

Pacific Semiconductors, Inc.
10451 West Jefferson Blvd.
Culver City, Calif.
Attn: H. Q. North

Union Carbide Corp.
Parma Research Laboratory
P. O. Box 6116
Cleveland 1, Ohio
Attn: R. G. Breckenridge
Library

Patterson, Moos
Div. of Universal Winding Co., Inc.
90-29 Van Wyck Expressway
Jamaica 18, New York
Attn: Library
H. C. Lieb

Philco Corp.
Tioga & C Sts.
Philadelphia 34, Pa.
Attn: Research Library

Philips Laboratories
Irvington-on-Hudson, New York
Attn: Library
E. S. Rittner

Polaroid Corp.
730 Main Street
Cambridge 39, Mass.
Attn: R. Clark Jones

Radio Corp. of America Laboratories
Princeton, N.J.
Attn: Library
S. Larach

Thomas A. Edison Research Lab.
East Orange, N.J.
Attn: Research Library
D. H. Howling

General Ceramics Corp.
Keasbey, N.J.
Attn: E. J. Hurst

General Electric Research Lab.
Schenectady, N.Y.
Attn: L. Apker
John R. Eshbach
R. W. Schmitt

General Motors Technical Center
Physics Dept., Research Laboratories
12 Mile and Mount Roads
Warren, Michigan
Attn: Carl E. Bleil
Robert Herman

General Telephone and Electronics Laboratories, Inc.
Bayside 60, New York
Attn: P. H. Keck
S. Mayburg
Library

International Business Machines Corp.
Research Center
Yorktown Heights, New York
Attn: J. Samuel Smart
L. P. Hunter
J. F. Woods
T. R. McGuire
Frank Stern

ITT Laboratories
3702 E. Pontiac Street
Fort Wayne, Indiana
Attn: Donald K. Coles

P. R. Mallory & Co., Inc.
3029 E. Washington St.
Indianapolis 6, Indiana
Attn: Margaret Holtman, Librarian

Raytheon Mfg. Co.
1st Avenue
Needham, Mass.
Attn: R. J. Carney

Raytheon Mfg. Co.
150 California St.
Newton, Mass.
Attn: Library

Santa Barbara Research Center
Goleta, Calif.
Attn: Library
D. E. Bode
R. M. Talley

Shell Development Co.
P. O. Box 481
Houston, Texas
Attn: D. R. Lewis

Shockley Transistor
Unit of Clevite Transistor
391 S. San Antonio Rd.
Mount View, Calif.
Attn: Library

Texas Instruments Inc.
Central Research & Engineering
P. O. Box 1079
Dallas 21, Texas
Attn: C. D. Mouser, Tech. Inf. Services
J. R. Macdonald
Apparatus Div.
R. L. Petritz

CATALOGING INFORMATION FOR LIBRARY USE

BIBLIOGRAPHIC INFORMATION

	DESCRIPTORS	CODES		DESCRIPTORS	CODES
SOURCE	NOLTR	NOLTR	SECURITY CLASSIFICATION AND CODE COUNT	Unclassified - 36	UØ36
REPORT NUMBER	62 - 125	62Ø125	CIRCULATION LIMITATION		
REPORT DATE	July 1962	ØØ762	CIRCULATION LIMITATION OR BIBLIOGRAPHIC		
*			BIBLIOGRAPHIC (SUPPL., VOL., ETC.)		

SUBJECT ANALYSIS OF REPORT

DESCRIPTORS	CODES	DESCRIPTORS	CODES	DESCRIPTORS	CODES
NOL Applied Phys. Dept.	APDN	Equation	EQUA	Photography	PHOT
Solid State	SOLS	Magneto	MAGE	Metals	META
Physics (Research)	PHYSR	Elastic	ELAS	Alloys	ALLO
1961	1961	Interactions	INAC	Nickel	NICK
N.O.L.	NOLA	Acoustics	ACOU	Tin	TINE
Semiconductors	SEMC	Silicon	SILC	Nitinol	NTIN
Semiconductors (Properties)	SEMCP	Oxide	OXID	Tellurides	TELL
Optical	OPTI	Chemical	CHEM	Spin	SPIN
Electrical	ELEC	Bonds	BOND	Lattice	LATT
Lead	LEAD	Laser	LASE	Rare Earth	RARA
Salts	SALT	Mechanisms	MECH	Materials	MATE
Boltzmann	BOLZ	High Speed	HIGS	Physics	PHYS

Naval Ordnance Laboratory, White Oak, Md. (NOL technical report 62-125)
SOLID STATE RESEARCH OF THE APPLIED PHYSICS DEPARTMENT FOR THE YEAR 1961(U). 16 July 1962. 52p. illus., tables, graphs.
UNCLASSIFIED

Emphasis placed upon optical and electrical properties of lead salt semiconductors and work on SnTe. Surface transport studies of semiconductors clarified by reformulation of Boltzmann equation. Magnetoelastic interactions constituted important effort during year. Acoustic investigations of SiO_2 were continued with reference to Si-O-Si bond that included relationships between specific heat and temperature dependence of elastic moduli of SiO_2 glass. Laser mechanisms studied by use of high speed photography. New alloy, Nitinol, revealed many unusual properties. Certain device applications of solid state principles reported.

1. Solid state physics
2. Semiconductors
3. Lasers
4. Materials, Magnetic
5. Nitinol
6. Silicon oxide
7. Lead telluride
8. Tin telluride
9. Optics
I. Title

Abstract card is unclassified

Naval Ordnance Laboratory, White Oak, Md. (NOL technical report 62-125)
SOLID STATE RESEARCH OF THE APPLIED PHYSICS DEPARTMENT FOR THE YEAR 1961(U). 16 July 1962. 52p. illus., tables, graphs.
UNCLASSIFIED

Emphasis placed upon optical and electrical properties of lead salt semiconductors and work on SnTe. Surface transport studies of semiconductors clarified by reformulation of Boltzmann equation. Magnetoelastic interactions constituted important effort during year. Acoustic investigations of SiO_2 were continued with reference to Si-O-Si bond that included relationships between specific heat and temperature dependence of elastic moduli of SiO_2 glass. Laser mechanisms studied by use of high speed photography. New alloy, Nitinol, revealed many unusual properties. Certain device applications of solid state principles reported.

1. Solid state physics
2. Semiconductors
3. Lasers
4. Materials, Magnetic
5. Nitinol
6. Silicon oxide
7. Lead telluride
8. Tin telluride
9. Optics
I. Title

Abstract card is unclassified

Naval Ordnance Laboratory, White Oak, Md. (NOL technical report 62-125)
SOLID STATE RESEARCH OF THE APPLIED PHYSICS DEPARTMENT FOR THE YEAR 1961(U). 16 July 1962. 52p. illus., tables, graphs.
UNCLASSIFIED

Emphasis placed upon optical and electrical properties of lead salt semiconductors and work on SnTe. Surface transport studies of semiconductors clarified by reformulation of Boltzmann equation. Magnetoelastic interactions constituted important effort during year. Acoustic investigations of SiO_2 were continued with reference to Si-O-Si bond that included relationships between specific heat and temperature dependence of elastic moduli of SiO_2 glass. Laser mechanisms studied by use of high speed photography. New alloy, Nitinol, revealed many unusual properties. Certain device applications of solid state principles reported.

1. Solid state physics
2. Semiconductors
3. Lasers
4. Materials, Magnetic
5. Nitinol
6. Silicon oxide
7. Lead telluride
8. Tin telluride
9. Optics
I. Title

Abstract card is unclassified

Naval Ordnance Laboratory, White Oak, Md. (NOL technical report 62-125)
SOLID STATE RESEARCH OF THE APPLIED PHYSICS DEPARTMENT FOR THE YEAR 1961(U). 16 July 1962. 52p. illus., tables, graphs.
UNCLASSIFIED

Emphasis placed upon optical and electrical properties of lead salt semiconductors and work on SnTe. Surface transport studies of semiconductors clarified by reformulation of Boltzmann equation. Magnetoelastic interactions constituted important effort during year. Acoustic investigations of SiO_2 were continued with reference to Si-O-Si bond that included relationships between specific heat and temperature dependence of elastic moduli of SiO_2 glass. Laser mechanisms studied by use of high speed photography. New alloy, Nitinol, revealed many unusual properties. Certain device applications of solid state principles reported.

1. Solid state physics
2. Semiconductors
3. Lasers
4. Materials, Magnetic
5. Nitinol
6. Silicon oxide
7. Lead telluride
8. Tin telluride
9. Optics
I. Title

Abstract card is unclassified